Detection and Classification of Reaching and Grasping Motions for Brain-Computer Interface Applications

Biomedical Engineering & Informatics, Aalborg University
4^{th} Semester, Master Thesis

Ardalan A. Wais
Group 18gr9440

Aalborg University
School of Medicine and Health, SMH
Fredrik Bajers Vej 7A
DK-9220 Aalborg Øst

School of Medicine and Health
Fredrik Bajers Vej 7
DK-9220 Aalborg Ø
http://smh.aau.dk

AALBORG UNIVERSITY
STUDENT REPORT

Title:
Detection and Classification of Reaching and Grasping Motions for Brain-Computer Interface Applications

Theme:
Master's Thesis

Project Period:
Autumn Semester 2018

Project Group:
18gr9440

Participant(s):
Ardalan A. Wais

Supervisor(s):
Strahinja Dosen

Copies: 1

Page Numbers: 51

Date of Completion:
January 03, 2019

Abstract:

Background: People suffering from major motor deficiencies such as amyotrophic lateral sclerosis (ALS) can not benefit from usual assistive devices since these devices require some motor function. Therefore a brain-computer interface could be of help to provide an assistive device which do not require voluntary movements, but motor intention. This would help the ALS patients to regain as much independence as well as improving their quality of life. In the present study, a random forest (RF) model was developed in order to detect and classify reaching and grasping motions for control of a robotic arm.
Methods: The RF model was developed using data sets across three sessions which consisted of 1)performing reaching movement 2) performing grasping movement and 3) performing both reaching and grasping movements. EEG signals were recorded across nine channels and motor-related potentials (MRCP) were extracted.
Results: The results showed it was possible to detect both reaching and grasping movements with an average true positive rate(TPR) of respectively 90.63% ± 18.43% (mean ± standard deviation) and 84.72% ± 21.76% across seven subjects. The classification accuracy for reaching and grasping based on two subjects which participated in session two were an average of 74.82% ± 11.44% across both subjects.
Conclusion: By using a RF model, it was possible to detect and classify reaching and grasping motions. The results shows promising results of utilizing a MRCP-based BCI for ALS patients to control a robotic arm.

Preface

This master thesis in Biomedical Engineering & Informatics at Aalborg University was conducted in the period from September 3rd, 2018, to January 3rd, 2019. The focus of the study was classification and detection of reaching and grasping motions for a brain-computer interface. The study included methods from machine learning and signal processing and may be of interest to anyone with an interest within the field of Biomedical Engineering & Informatics and brain-computer interfaces.
I would like to thank my supervisor, Strahinja Dosen, for a competent and useful supervision that helped completing this master thesis.

Reading guide

Citations will be made according to the Vancouver method, e.g. [1]. If the citation is referred to a whole section, the citation is placed after the period of the last sentence. However, if the citation is referred before the period, it refers to the single sentence. Furthermore, citations can be referred to within a sentence, which refers to the given statement.

Aalborg University, January 03 2019

Ardalan Wais
<awais13@student.aau.dk>

Contents

1 | Introduction

Neuromuscular disorders affects the nervous system in such way that a person can lose their ability to communicate and interact with their environment. Amyotrophic lateral sclerosis (ALS), multiple sclerosis, brain or spinal cord injury and numerous other neuromuscular diseases impair the neural pathways that control the muscles in the human body. An impairment of the neural pathways can result in motor disabilities, leaving the person unable to do voluntary movements.[1, 2]
ALS is a rare progressive neuromuscular disease where neurons are dying, and there are currently no treatment available. Patients suffering from ALS may have to accept artificial respiration and as the disease progresses it will eventually lead to death.[3]. In Denmark it is estimated that around 400 patients are suffering from ALS, whereas in the U.S more than 2 million is affected. The worldwide prevalence of ALS has not been estimated, but the prevalence in European countries is estimated to be 2-3 people per year per 100.000 citizens.[4]. The restoration of communication and interaction with the external environment is crucial for ALS and other patients suffering from neuromuscular disorders. Due to technological advancements, patients with severe motor disabilities are able to interact with their surroundings using brain-computer interfaces (BCI). BCI do not require any voluntary motor functions and can be controlled by using electroencephalography (EEG). BCI makes it possible for patients suffering from severe motor disabilities to interact with external devices such as writing letters using a computer or controlling a robotic arm.[1, 5] These applications among others make BCI a suitable solution for patients suffering from ALS to regain as much independence as possible and simultaneously improve their quality of life by utilizing a robotic arm that can perform reaching and grasping. The aim of this thesis is therefore to develop a detection and classification model that can be used for the control of an assistive device using reaching and grasping movements.

2 | Problem Analysis

To understand how electrophysiological signals from the brain occur, the brain's structure and functionality will first be investigated together with a focus on ALS' impact on voluntary movements. Afterwards a description of the current recording methods to obtain the brain signals will be presented. The current studies in the field of BCI will afterwards be presented and at last the aim of this thesis.

2.1 Anatomy and Physiology of the Brain

The central nervous system (CNS) is a part of the nervous system and includes the brain and the spinal cord. It is the most complex part of the human body and has the ability to produce actions through motor commands and to form memories and thoughts through interactions between a network of neurons in the brain. The brain can be divided into three major parts; the cerebrum, cerebellum, and the brain stem. The cerebrum is the largest part of the brain and controls all voluntary movements together with the cerebellum.[6]
Cerebrum can furthermore be divided into two brain hemispheres respectively right and left hemisphere. The muscles to the left of the body are controlled by the right hemisphere and the left hemisphere controls the muscles in the right side of the body. In each hemisphere the cerebral cortex is categorized into four lobes; frontal lobe, parietal lobe, temporal lobe and occipital lobe, which are illustrated in figure 2.1 and described in table 2.1.[6, 7]

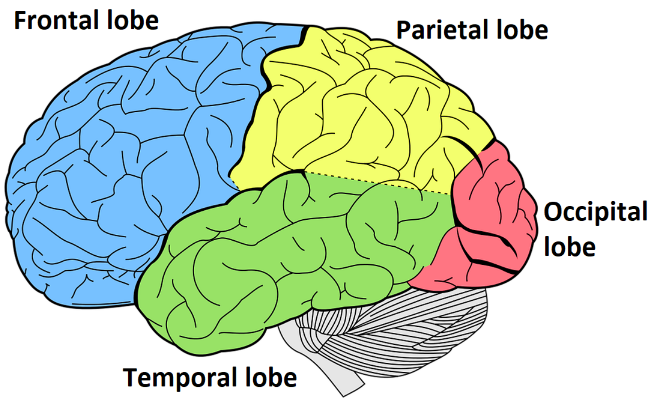

Figure 2.1: The figure illustrates the four lobes of the brain, which are the frontal, parietal, temporal and occipital lobe. Modified from[8]

Table 2.1: An overview of the different lobes of the brain, respectively, frontal, parietal, temporal and occipital lobe.

Frontal lobe	The frontal lobe is located at the front of the brain and is associated with motor skills and speech production. At the back of the frontal lobe lies the motor cortex which is involved in control and execution of voluntary movements of skeletal muscles.[6]
Parietal lobe	The parietal lobe is associated with processing sensory information. It responds to stimuli such as temperature and pain.[6]
Temporal lobe	The temporal lobe is the location of the auditory cortex which is the center of interpreting language and sound and perception of olfactory stimuli.[6]
Occipital lobe	The visual cortex is located in the occipital lobe at the back of the cerebrum and is associated with interpreting visual information from the retina.[6]

2.1.1 Amytrophic Lateral Sclerosis and Its Impact on Voluntary Movements

ALS is a neurodegenerative disease which is characterized by a progressive loss of upper and lower motor neurons. Upper motor neurons are responsible for initiating voluntary movements and are located in the primary motor cortex in the frontal lobe of the brain. The general structure and function of a neuron is further described in appendix A. When a voluntary movement is initiated, upper motor neurons will active the lower motor neurons located in the spinal cord which activates the muscles. Axons of upper motor neurons originate in the motor cortex and are connected to the spinal cord whereas axons of the lower motor neurons originate in the spinal cord and are connected to the skeletal muscles.[6] An organization of these motor neurons and the motor cortex can be explained through somatotopy. These motor neurons originating from the motor cortex are responsible for the motor control of specific body parts and is represented in specific cortical regions, which are illustrated in figure 2.2. The figure illustrates that the arm and the hands are among the largest representation.

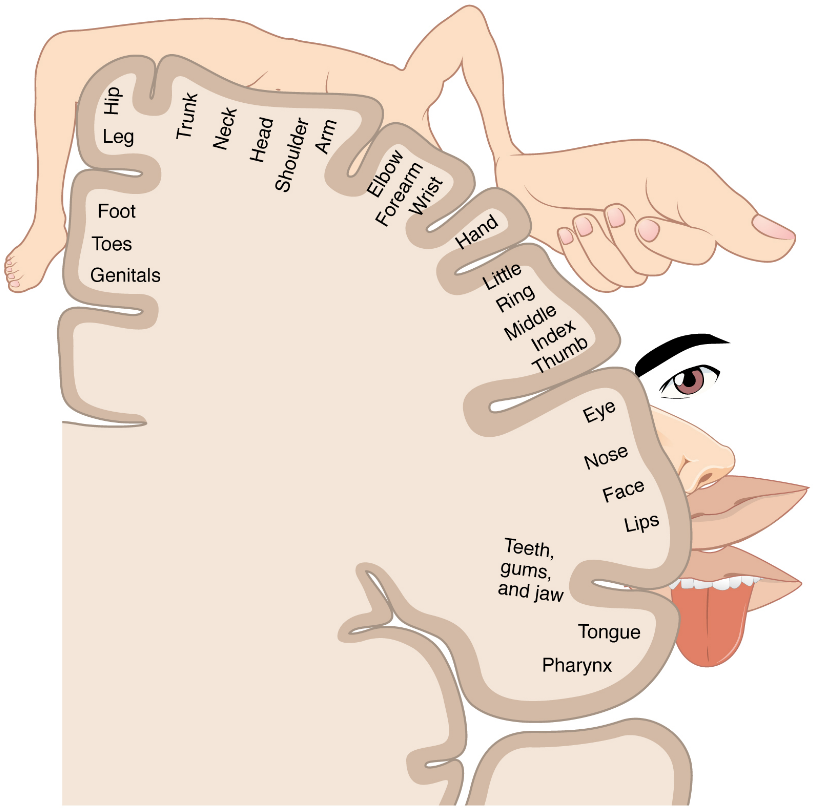

Figure 2.2: A representation of the different body parts, which the motor cortex are responsible for.[9]

When a dysfunction of generating action potentials in upper or lower motor neuron occurs, the targeted skeletal muscles can not be activated. Patients with major motor deficiencies will therefore lose the ability to execute voluntary movements[10]. This is the case for ALS patients as they progressively lose their ability to execute voluntary movements. The most common phenotype is limb-onset ALS where the main characteristics are a progressive loss of both upper and lower motor neurons. Seventy percent of ALS cases are limb-onset, where the disease affects the upper and lower limbs, 25% of the cases are bulbar onset, which impacts the cranial nerves, making it difficult for the patient to swallow and speak. It is also possible that the disease starts as limb-onset ALS and then later spreads to the cranial nerves. Typical symptoms of ALS are weakness of the extremities, dysarthria and dysphagia.[11, 10] Five to ten percent of ALS cases are familial, meaning that there is evidence of genetic inheritance of

ALS. However in addition to genetics, assumptions of environmental factors such as smoking has been associated with increasing risk of ALS.[11, 12] Furthermore excitotoxicity has been taken into consideration as a possible cause of neurodegeneration. Excitotoxcity is a process where neurons are damaged due to an excessive release of neurotransmitters. The primary neurotransmitter that are released in the neuron synapses in the brain is glutamate. If the receptors that binds glutamate are overactivated due to the excessive amount of glutamate, it can potentially cause neurodegeneration of the motorneurons.[11]
As the disease progresses, patients suffering ALS will have difficulty in executing voluntary movements, including reaching and grasping movements. Therefore an assistive device with the use of BCI could be of help.

2.2 Brain-Computer Interface

A BCI is a communication system that enables the human to communicate and/or interact with its surroundings without the use of voluntary movements, which makes it a useful tool for people suffering from ALS.
There are two types of BCI systems which are known as synchronous and asynchronous BCI.[5]

- Synchronous BCI (cue-paced BCI): Acts upon a cue stimulus. In this approach, brain signals are analyzed only in a predefined time frame, allowing the subject to create artifacts such as blinking and swallowing since it would not be affected by the analysis.[5]
- Asynchronous BCI (self-paced BCI): Does not act on a cue stimulus. It continuously analyzes the brain signals, which makes the BCI system more sensitive to artifacts e.g. eye movements or blinking. Although it is more preferable as it allows the user to use the system whenever it is wished.[5]

Before the 2000's, BCI technology was not desired due to the resolution of the signal. The complications also lied within the computational power of the BCI systems, as it require real-time data acquisition. However, due to technological advancements, investigation of BCI has led to an usage of BCI systems and it is being utilized by people with severe motor disabilities, among other dysfunctions, to recover their motor functions through neurorehabilitation programs.[5, 13] Most rehabilitation programs for patients with motor deficiencies includes motor learning, where patients learn to train their motor function. This requires some motor functions in order to work.[14] ALS patients with no motor control at all, can not benefit from these rehabilitation programs which is why a BCI system can be used for ALS patients for control of a robotic arm to perform reaching and grasping.

2.2.1 Signal Acquisition of Brain-computer Interfaces

Two methods are available for recording of the brain activity for BCI systems, which are electrophysiological and hemodynamic methods. Electrophysiological signals can be obtained due to neuron activity. When neurons exchange information through neurotransmitters, they are generating action potentials. These action potentials are ionic currents that flow through the cell membrane and thereby creates a dipole between the two endpoints of a neuron. Electrophysiological signals can be obtained through electroencephalography (EEG), electrocorticography (ECoG), intracortical neuron activity and magnetoencephalography (MEG). ECoG measures the neuron activity using electrodes that are surgically implanted on the motor cortex.[5] Intracortical neuron activity measures the neuron activity by implanting electrodes inside of the motor cortex. Three types of signals can be obtained from intracortical neuron activity which are, single-unit activity (SUA) which measures activity of a single neuron, multi-unit activity (MUA) which measures activity of multiple neurons and local field potential (LFP) which is a composite signal based on input of the activity from multiple neurons.[5] MEG measures the magnetic field generated by ionic currents. During neuron activity, the neurons will need more energy than the inactive neurons. The blood will therefore release glucose in order to provide more energy to the active neurons. These changes in the concentration of oxyhemoglobin can be obtained through neuroimaging methods such as functional magnetic resonance imaging (fMRI) and near-infrared spectroscopy (NIRS). fMRI measures the changes in the concentration of the oxyhemoglobin to locate active regions in the brain through electromagnetic fields. NIRS uses infrared light to penetrate the skull in depths around 1-3 cm to measure the changes in oxyhemoglobin. Table 2.2 provides an overview of the above mentioned methods and their differences in temporal resolution, spatial resolution, the methods risk and their portability.[5]

Table 2.2: The table shows the different types of electrophysiological and hemodynamic methods of recording brain activity and their spatial resolution. Furthermore it gives an overview of whether the methods are non-invasive or invasive as well as if the method is portable. The temporal resolution is given in seconds (s) and the spatial resolution is given by milimeters (mm).

Method	**Activity response**	**Temporal resolution (s)**	**Spatial resolution (mm)**	**Risk**	**Portable**
EEG	Electrophysiological	0.05	10	Non-invasive	✓
ECoG	Electrophysiological	0.003	1	Invasive	✓
Intra-cortical neuron activity	Electrophysiological	0.003	0.05 (SUA) 0.1 (MUA) 0.5 (LFP)	Invasive	✓
MEG	Magnetic	0.05	5	Non-invasive	X
fMRI	Metabolic	1	1	Non-invasive	X
NIRS	Metabolic	1	5	Non-invasive	X

A portable BCI system for patients with severe motor disability is preferred as it would help the patients to use the system freely with no restrictions in regards to location. For instance if they were needed to control a wheelchair, the system would preferably be portable. ECoG and intracortical neuron measuring have higher spatial resolution since they are surgically implanted on the cerebral cortex, giving the method an advantage to measure neurons with maximal signal-to-noise ratio. However, it is more practical to use EEG to measure neuron activity due to its advantages of being non-invasive, cheap, portable and a low temporal resolution.[5, 13] EEG is the most popular recording method due to its non-invasive procedure, however there is a trade-off between signal quality and the recording method. ECoG or intracortical neuron measuring have high spatial resolution, meaning they provide information directly related to the neurons. However, they are invasive methods. EEG signals have low spatial resolution since they are recording across the scalp. They are poor quality signals as they are small and can often be mistaken for noise. However, preprocessing methods can be applied to improve the signal quality and due to its non-invasive procedure and its temporal resolution, it will therefore be used to obtain the brain activity in this study.[5]

2.2.2 Control Signals of Brain-computer Interfaces

In order to control and interact with a BCI, several phenomena can be extracted and decoded from the EEG signal which are used for the BCI to interpret the intention of the user. The extracted phenomena can be divided into two categories: evoked potentials and event-related potentials (ERP). [13, 5]

Evoked Potentials

Evoked potentials are the measured brain response related to external stimuli such as visual stimulus and auditory stimulus. The most common types of evoked potentials are steady-state evoked potentials (SSEP)
SSEP are signals related to periodic external stimulus for instance a LED flickering while observed by the subject or a periodic audio stimulus. Such stimulations will impact the brain signals frequency to reach the same frequency of the flashing LED and thereby harmonize with the frequency of the LED's or of auditory stimulus. If the frequency of the stimulation is >3.5 Hz it is called a 'steady-state', whereas stimulation frequencies <3.5 Hz are called 'transient' visual evoked potentials[13]. Steady-state visual evoked potentials (SSVEP) are a SSEP that are generated through a repetitive visual stimuli of LED's at a specific frequency typically between 6-30 Hz. The visual stimuli will generate a potential that has the same frequency of the LED, for instance if a LED is flashing at 15 Hz, the SSVEP can be detected at 15 Hz in the frequency spectrum of the EEG signal.[5, 13]. Figure 2.3 illustrates the SSVEP detected when a subject stares at a LED flickering at 15 Hz. The second and third order harmonics for the 15 Hz SSVEP is also visible in the figure.

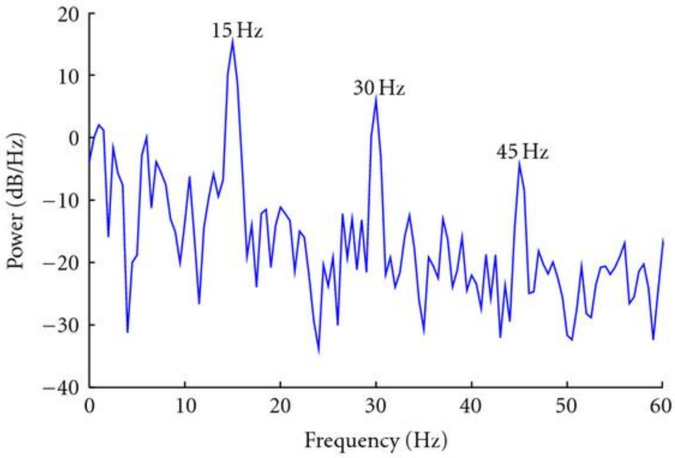

Figure 2.3: A power spectrum of a recorded EEG signal. The SSVEP is being detected at 15 Hz together with its second and third order harmonic frequencies, respectively 30 Hz and 45 Hz.[15]

Event-related Potentials

ERP are the measured brain response related to cerebral activity in regards to sensory and cognitive processes. The commonly used ERPs are sensorimotor rhythms (SMR) and movement-related cortical potentials (MRCP). SMR is made up by osciliations in the brain activity of the alpha (8-13 Hz) and beta band (13-30 Hz). SMR are frequency bands located over the motor cortex. Therefore the power of the signal in the respective bands changes when they are related to voluntary motor tasks. These modulations in the power are associated with neuronal structure underlying the motor cortex and can be seen in the EEG oscillations, known as event-related synchronization (ERS) and event-related desynchronization (ERD).[5, 16] Both can be measured at the same time when performing a motor task, where ERD is indicated as a suppression within the alpha band and beta band over the contralateral sensorimotor cortex. Furthermore, the ERS increases within the alpha and beta band over the ipsilateral sensorimotor cortex.[16] Although the actual movement execution is not required to generate the responses and can be done through motor imagery, where the variation in the signals occurs due to motor imagery of the arm or leg. Motor imagery is a term for imagining a movement without executing it.[5, 13]
MRCPs are a slow cortical potential (SCP) and are found between 0.1-5 Hz in the frequency range. It is present in the EEG signal as a negative shift that starts 2 seconds before the execution or imagination of a voluntary movement. The negative shift represents increased neuronal activity, which can be related to the neuronal activity before initiating the voluntary movement or motor imagery. Due to MRCP's being directly related to movement, they can be used as a control signal to detect movement.[17]
Figure 2.4 illustrates the representation of a MRCP. A MRCP consists of a Bereitschafts potential (BP) followed by a motor potential (MP) and a motor monitoring potential (MMP).

BP is considered to be related to motor preparation and is the first part of the MRCP which begins 2 seconds before movement onset. The BP2 in figure 2.4 is also known as the late BP, which is a steep negative slope that occurs approximately 400 ms before movement onset. The negative steep of the late BP can be influenced by factors such as the complexity of the movement. MP and MMP are respectively related to movement execution and performance. [17, 18]

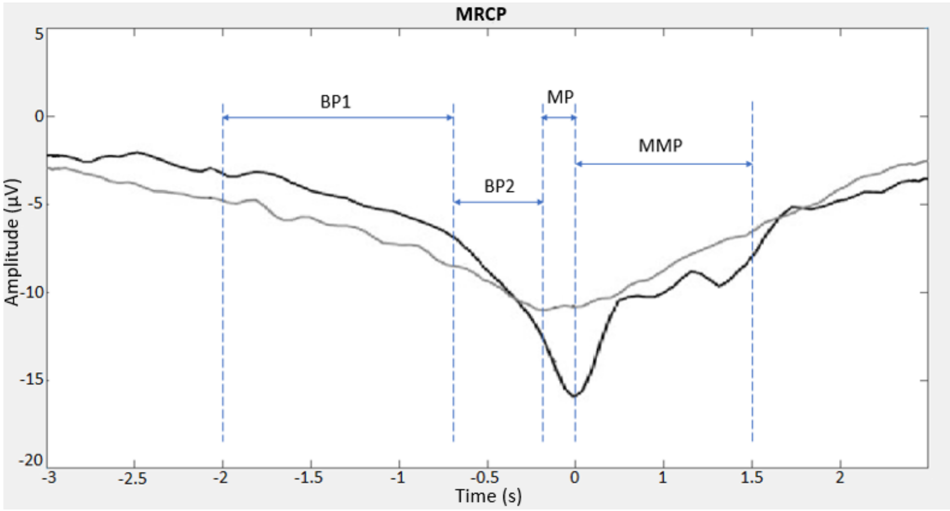

Figure 2.4: A MRCP and its components with early and late BP, MP and MMP. The black line represents a MRCP for an executed movement, and the gray line represents a MRCP related to an imaginary movement. Modified from [17].

Several of these control signals can be used to interpret information of voluntary movements in patients with ALS. An understanding of the current research field is needed to clarify which of these phenomena can be extracted for motor-related tasks such as controlling an external device e.g. robotic arms.

2.3 State of the Art

There are no golden standards for which phenoma that are best suited, when developing a BCI. This section will give an overview of the current studies of BCI systems that extracted SSEP's and ERP's in order to control an external device for grasping and reaching, which can be utilized by patients with severe motor disabilities.
A number of approaches for controlling BCI systems have been proposed. These studies used different control signals in order to classify or detect voluntary movements. A study by Müller-Putz et al. [19] presented a SSVEP-based BCI for control of an electrical prosthesis. Four LEDs were mounted on the hand prosthesis where each LED had its own function; turn left/right and open/close. To produce these actions, the subjects were required to have direct eye contact on the desired LED to turn on the switch. Results showed three of the four subjects had classification accuracies from 74% to 88% where the fourth subject had

a classification accuracy of 44%. The study indicates that SSVEP-based systems can be used instead of motor-related control signals for control of a robotic arm. SSVEP-based BCI systems are very often used due to low training time, and the number of choices are high (more than four choices). However, SSVEP-based BCI systems requires external stimuli. This might not be optimal as subjects can get fatigued of the flickering LED stimulation. Furthermore it is not practical to look at LEDs to control a prosthesis. Control signals related to motor-related movements would therefore be more preferable than evoked potentials.
A study by Pfurtscheller et al. [20] investigated an ERS/ERD-driven BCI system to control a hand orthosis for grasping in a high-level spinal cord injury patient. The study consisted of 160 trials in which the patient was asked to imagine either left/right movement of the hand or the legs. A classification accuracy of 65% was achieved by imagining right vs. left arm movements to open and close the hand orthosis. However, this accuracy was improved by using various strategies. In the last training sessions, the strategy was for the subject to imagine movement in both legs and in the right arm. Motor imagination of both legs would close the hand and motor imagination of right hand would open the hand orthosis. This improved the classification accuracy to 95%. Topological measurements of the subject's brain showed changes in the motor cortical area, indicating neuroplasticity changes in the motor cortex which was induced through the training sessions.[20] SMR can be used as a control signal to detect grasping. However, SMR requires a lot of training before any physical or functional changes can be seen[21]. Another approach to utilize a BCI through motor imagery without weeks of training could be a MRCP-based BCI. In a study presented by Niazi et al.[17], detection of MRCPs was investigated in both healthy and stroke subjects. The proposed algorithm was able to detect movement execution and motor imagination. Movement execution in healthy subjects had a true positive rate (TPR) of 82% ± 7.8% and motor imagination for both healthy and stroke subjects had a TPR of 64% ± 5.33% and 55% ± 12.01%. The study showed promising results for detection of MRCPs without many training sessions. A study by Xu et al.[22] also presented a MRCP-based BCI system. Nine healthy subjects performed both motor execution and motor imagination of lower limbs. The mean TPR for both motor execution and motor imagination combined was 79% ± 11% indicating it was possible to detect MRCPs in healthy subjects only. A study by Bhagat et al.[23] extracted MRCPs to control a MAHI Exo-II upper limb exoskeleton for extension and flexion of the elbow. Four stroke patients were enrolled in the study with the purpose of detecting motor intention of flexion and extension of the elbow. The study obtained an overall TPR of 64.86% ± 18.35% for motor intention across all subjects. However, one subject managed to achieve a TPR of 91% ± 10%. The study indicates MRCPs can be extracted and utilized by a BCI for control of an upper limb exoskeleton.

2.4 Project Statement

Patients suffering from major motor deficits caused by ALS will progressively lose their abilities to execute voluntary movements. BCI has opened up the opportunities to help patients with major motor disabilities to control hand and arm exoskeletons. When working with BCI systems related to motor control, MRCP's are relevant as they are directly related to motor movement and requires no training to be generated. Decoding these control signals can therefore potentially help ALS patients and other patient groups suffering from major motor dysfunctions, to utilize a BCI for control of a robotic arm. This project sets out to develop a MRCP-based BCI for patients suffering ALS in order to control reaching and grasping of a robotic arm to help them regain as much independence in their everyday life as possible. This leads to the aim of the project:

How can a MRCP-based BCI system be developed in order to detect and classify reaching and grasping for rehabilitation purposes to help patients suffering from ALS?

3 Methodology

In this chapter each step of the model implementation will be presented. First the pipeline of the study, then the subsequent sections that explains the methods that were carried out in each step of the study design. The five sections are; signal acquisition, preprocessing, feature extraction, feature selection, classification and evaluation.

3.1 Study Design

A standard pipeline that can be applied to any classification problem, including BCI systems is illustrated in figure 3.1. The proposed pipeline divides the model in four steps which are preprocessing, feature extraction, feature selection, classification and evaluation.[5]

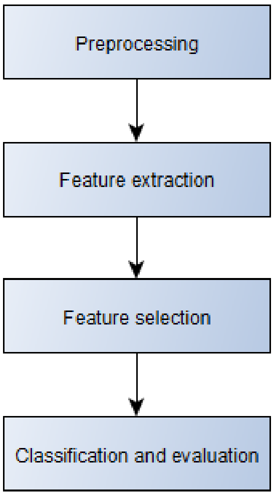

Figure 3.1: A flowchart representing a classic classification pipeline in order to achieve the classification model.

Two main objectives for the development of the model was pursued.

1. How well can the model detect reaching and grasping?

2. How well can the model classify reaching and grasping?

The first objective sets out to investigate how well reaching and grasping can be detected from a resting period. The second objective sets out to investigate how well the classifier can classify reaching and grasping.

3.2 Signal Acquisition

Data sets from seven subjects were previously recorded and provided in order to detect reaching and grasping. The recording took place over two sessions. The sessions took place on two different days. The first session consisted of executing only reaching movement and the second session consisted of only grasping movement. The subjects were seated in a chair with a table placed in front of them where the arm laid in a resting position. A computer monitor was placed in front of the subjects and was used to give directions to the subjects respectively, rest and focus. Figure 3.2 shows the experimental setup. During rest, the subject was allowed to swallow and blink, whereas during focus, the subject was instructed to withhold swallowing and blinking in order to avoid artifacts while performing either reaching or grasping for three seconds. The movement was executed after a cue was presented on the screen during the focus state. After performing the movement, the subjects were resting for 5 seconds before executing the movement again. In total 60 movements were executed where a small break of 5 minutes were held after the first 30 movements. Each movement was instructed to be performed ballistically.

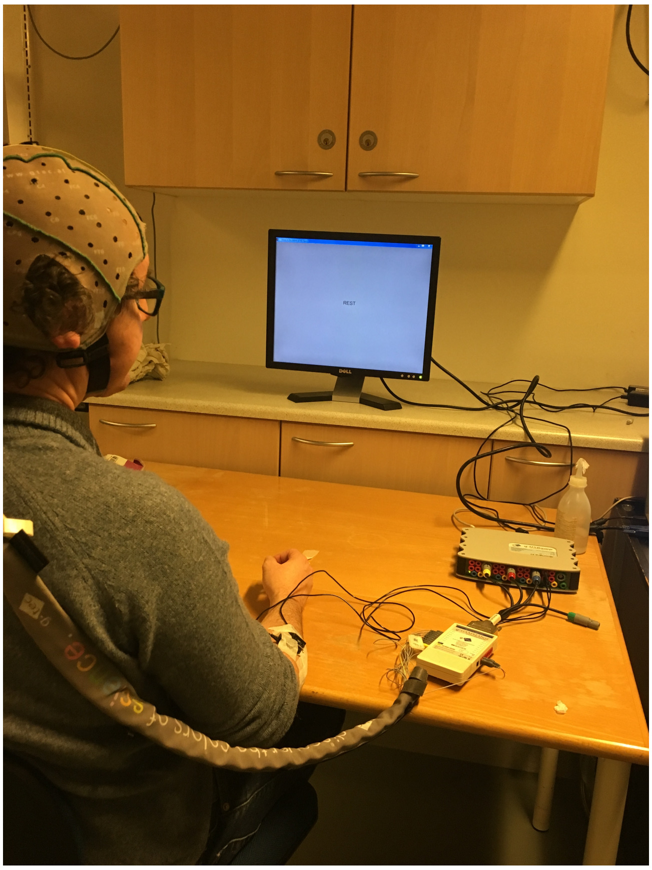

Figure 3.2: Experimental setup for one of the trials for a subject. The subject was seated in front of a monitor with the arm resting on the table. The monitor gave instructions to the subject, respectively rest and focus. During resting, the subject was allowed to blink and swallow, however when the text changed to focus, the subject was instructed to withold blinking and swallowing. During focus the subject performed either reaching or grasping movements when given a cue on the monitor.

The experiment in which the seven subjects were participating in, was carried out over two sessions, making the data sets unavailable to classify between reaching and grasping. The EEG signals would have different amplitude scaling and therefore biased due to both physical and experimental differences such as different mood or a different placement of the EEG cap. Two subjects were therefore enrolled to participate in a third session in order to obtain data sets that could be used to analyze how well a classifier can classify reaching and grasping. The same experimental protocol was followed as for the seven subjects who were recorded prior to this study, however in this session both reaching and grasping movements were performed.
The signals for all subjects were recorded from electrodes placed over the frontal, central and parietal lobe according to the 10-20 EEG system, which is illustrated in figure 3.3. Electrodes were mainly placed around the motor cortex since that area is related to motor related movements. The EEG signals were recorded across nine channels; F3, FC5, FC1,

T7, Cz, C3, CP5, CP1 and P3.

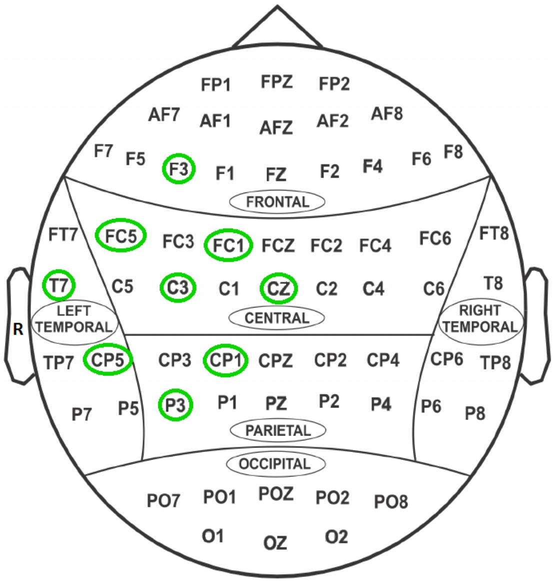

Figure 3.3: An extended version of the international 10-20 EEG system. The green markings indicate the nine channels used in the EEG recordings. The ground electrode was placed on the left ear, marked with 'R' and the reference electrode was FZ. Modified from [24].

EMG signals were recorded simultaneously with the EEG signals. Two recording electrodes of the type 720, AMBU A/S for the EMG signal were positioned on the belly of the muscle extensor carpi ulnaris on the right arm.
All signals were recorded using a sampling frequency of 1200 Hz.

3.3 Preprocessing

Preprocessing is a preliminary step towards achieving the fundamental data set for further processing. The preprocessing step aims to reduce the amount of noise contaminating the EEG signal, to remove outliers and to extract epochs containing the MRCPs from the filtered EEG signal. Figure 3.4 shows the different preprocessing steps for the data in this study.

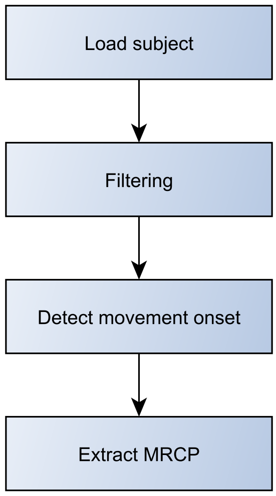

Figure 3.4: A flowchart showing the preliminary approach to obtain the dataset for further processing. The steps include filtering the signal from noise, detect movement onset and at last extracting the time window of the MRCPs.

3.3.1 Filtering

The EEG signals from all nine channels were bandpass filtered using a second order butterworth filter to prevent ripples in the passband and stopband. The filtering causes a phase shift in the signal. To prevent this problem, a zero-phase filtering was performed using the `filtfilt` function in MATLAB. The cut-off frequencies were 0.05 and 3 Hz which is the frequency range of the MRCP. These signals will be used for temporal feature extraction. Figure 3.5 shows an example of an EEG signal after applying the bandpass filter. Furthermore, to extract the features of the wavebands delta (0.01-3 Hz), theta (4-7 Hz), alpha (8-13 Hz), beta (16-31 Hz) and gamma (32-100 Hz), all nine channels were bandpass filtered according to the frequency ranges of their respective brainwave bands. The brain wavebands are further described in appendix B.

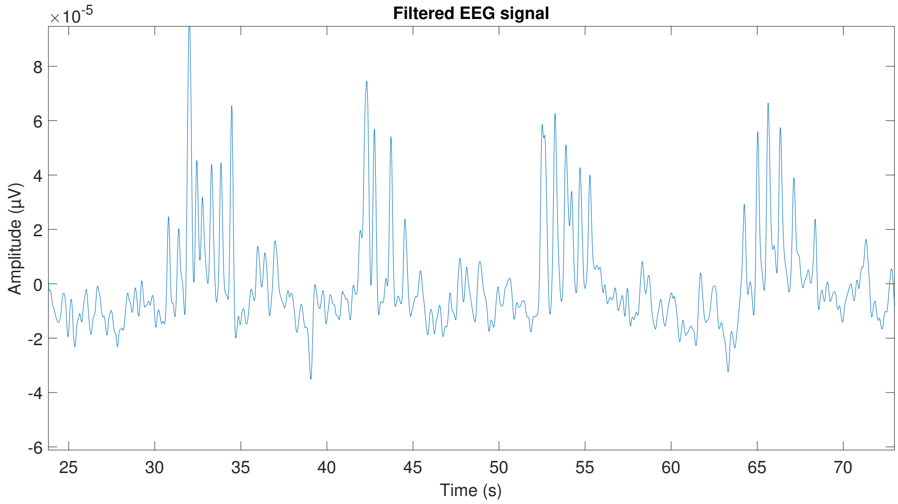

Figure 3.5: Filtered EEG signal using a second order butterworth bandpass filter with cut-off frequencies of 0.05 and 3 Hz.

In order to extract the epochs with the MRCPs, the movement onset in the EEG signals was located. The EMG signals were first filtered and corrected for DC-offset by applying a second order butterworth high-pass filter with a cut-off frequency of 10 Hz. Afterwards a full-wave rectification was obtained by converting the EMG signal to an output signal with only positive values. The absolute positive values were used in order to detect beginning of the EMG burst which is related to movement. After the full-wave rectification, the EMG signal was low-pass filtered using a second order butterworth filter with a cut-off frequency of 3 Hz to obtain the envelope of each EMG burst. Figure 3.6 shows the final outcome of the EMG signal after the preprocessing steps.

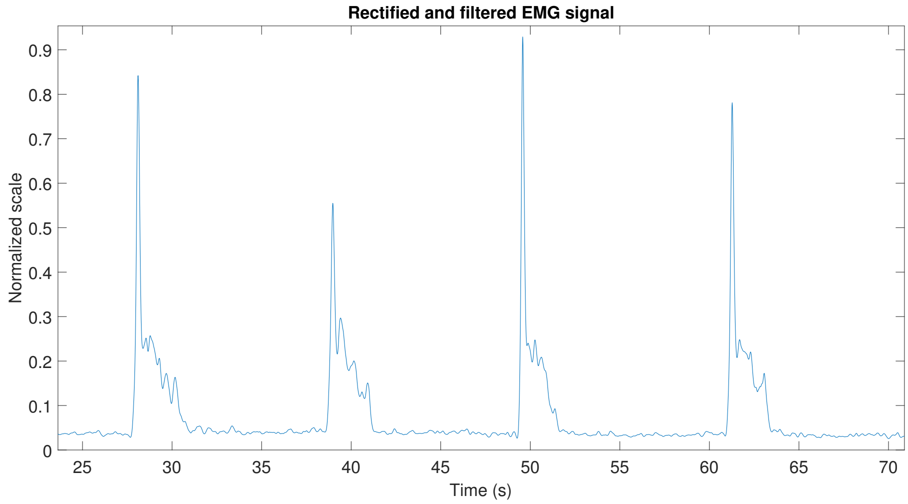

Figure 3.6: Low-pass filtering the rectified EMG signal results in a smoother signal with no noise. The beginning of each EMG burst can afterwards be used for the detection of the movement onset in the EEG signal. The y-axis is normalized from 0-1.

3.3.2 Movement Detection

A threshold was manually placed with the mouse cursor in each EMG signal to detect beginning of each EMG burst, which is illustrated in figure 3.7. This resulted in total of 60 EMG burst for each movement respectively reaching and grasping, which corresponds to the 60 movements which were executed in the sessions.

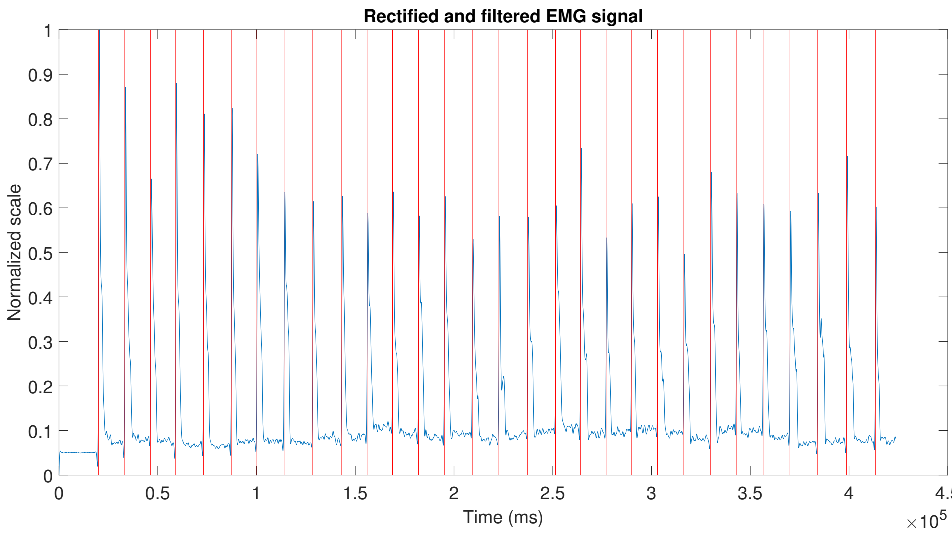

Figure 3.7: A manual threshold is placed with the mouse cursor. The start of each EMG burst above this threshold is detected. The red lines indicates the 30 bursts of EMG that are detected.

3.3.3 Extracting Epochs

After detecting the EMG peaks, the movement onset in the EEG signal was located by locating the maximum peak negativity as it was related to the motor potential component of the MRCP. Signal epochs were extracted 1 second prior the movement onset and 1 second after. Afterwards the epochs were extracted 1 second prior and after the maximum peak negativity as it was related to the MP component in the MRCP, which is illustrated in figure 3.8. 60 epochs of resting signal were also extracted which were epoch signals between 4 and 2 seconds prior to movement onset. In total 60 epochs of MRCPs from each reaching and grasping data set was obtained together with 60 resting epochs.[25]

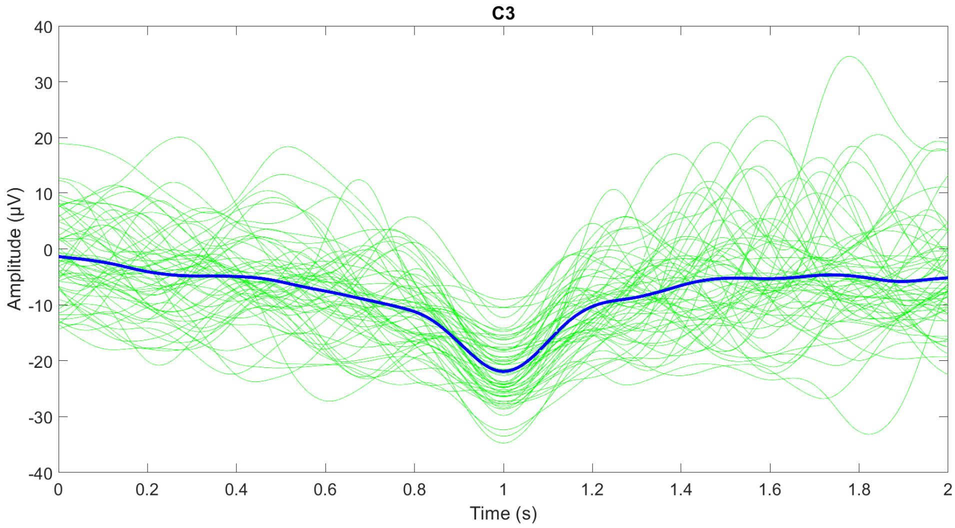

Figure 3.8: The extracted epochs 1 second prior and after the maximum peak negativity. The green signals are all the 60 epochs of the reaching movement extracted from channel C3. The blue line is the mean of all the 60 epochs for this channel.

Epoch signals based on the brainwave frequency bands were also extracted in order to be used for extracting features related to the brain rhythms for each respective band.[25] Figure 3.9 illustrates the epoch signals and the mean of the alpha frequency band for the reaching movement.

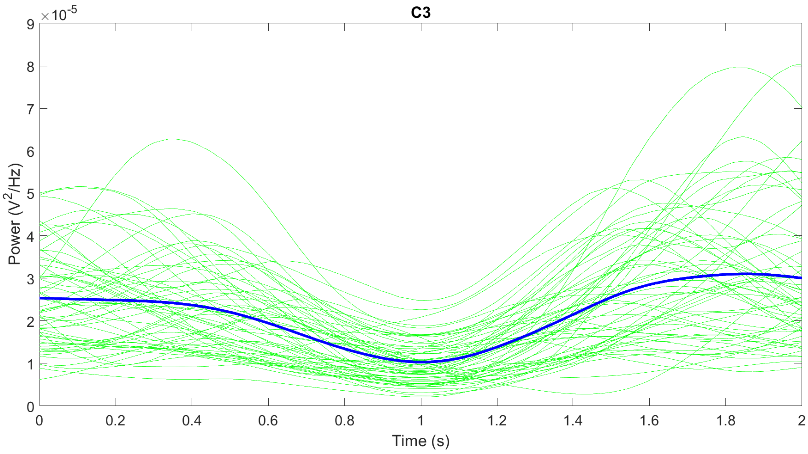

Figure 3.9: All the epochs 1 second prior and after the maximum peak negativity for the filtered EEG signal related to the alpha band. The desynchronization of the neurons is illustrated by the ERD supression centered at the MP.

During the experiment, some subjects were blinking while executing the movements, resulting in the epochs to be contaminated with EOG and were seen as outliers. These epochs were removed from the data set by a threshold that would remove the epoch if the peak-to-peak value were greater than 80 μV. The threshold value was empirically chosen by examining the epochs consisting of the blinking artifacts. Epoch signals which had values below -40 μV were also removed from further processing.

3.4 Feature Extraction

Features were extracted based on knowledge of the properties of a MRCP. In section 2.2.2 the components of the MRCP were described. It was illustrated that the first segment of the MRCP is a slow progressing negative slope which is the BP, followed by a steep negative slope which is characterized as BP2. The MP is the maximum peak negativity of the MRCP. To derive the properties of each component, the epochs were separated in six segments where two of them consisted of 1s and the remaining four consisted of 0.5s. These segments are expected to represent the components of the MRCP. Figure 3.10 illustrates the epoch signal which is divided in six segments. The time interval for each segment is given in table 3.1.

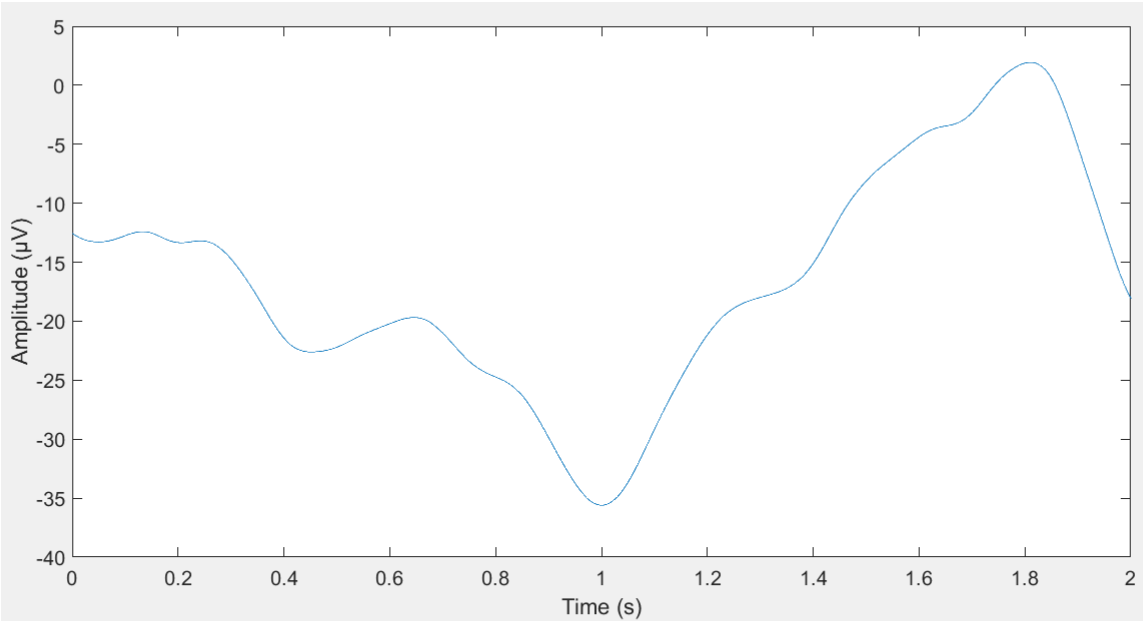

Figure 3.10: An example of an epoch signal in which features will be extracted. The length of the epoch signal is 2 seconds. Features will be extracted from six segments, where four segments will consist of 0.5 seconds, and two segments consisting of 1 second. In this way the whole epoch signal will be divided in order to capture each component of the MRCP.

Table 3.1: The time intervals of each segment related to the epoch signal. These segments will be used in the feature extraction, where features will be extracted based on the time intervals.

Segment	Time interval (seconds)
1	[0 - 1]
2	[0 - 0.5]
3	[0.5 - 1]
4	[1 - 1.5]
5	[1.5 - 2]
6	[1 - 2]

The MRCP has properties that can be explained in the time-domain. Furthermore, features can be extracted from the powerband of the respective brain wave bands, delta, theta, alpha, beta and gamma. Therefore temporal features and features related to the powerbands will be extracted.

3.4.1 Temporal Features

Temporal features has the purpose to extract statistical features of the MRCP. The components of BP1 and BP2 along with the MP and MMP can be quantified by measurements such as mean or the slope of each component. Therefore three temporal features were extracted from each segment: mean, variance and the linear slope of each segment.

3.4.2 Powerband Features

For the epoch signals that were low-pass filtered to each respective brainwave frequency, two features were extracted which were the mean and the slope of each segment. In total, 60 features related to their respective frequency band were extracted for each epoch signal per channel. Not all features represents the signal equally. It was therefore necessary to select a subset of features that represents the data set best and to avoid the curse of dimensionality.

3.5 Normalization and Feature Selection

Feature sets for each subject were prepared for feature selection and further processing by normalizing the feature set using the z-score which is given by equation 3.1. The z-score measures the distance of a data point x from sample data with mean $\overline{x}$ in units of the standard deviation S

$$z = \frac{(x - \overline{x})}{S} \tag{3.1}$$

Normalization is a recommended step in order to achieve a higher classification accuracy and it is required for some classifiers that the feature set is normalized.

Feature selection is a method which is often used in machine learning. The technique is used to reduce the feature dimensionality by selecting a subset features that represent the data set the best and remove redundant features which are seen as noise in the feature set.[5, 26] There are three methods for feature selection which are; filtering approach, wrapper and embedded methods. The proposed study used both the wrapper and embedded method.

Filtering approach is a simple method for feature selection, which is done without taking the model into consideration. A filter approach could be to remove correlated features or remove features based on a t-test, where features which do not differ significantly will be removed.[26]

Wrapper methods are machine learning algorithms that aims to minimize a loss function or the classification error by selecting features iteratively e.g. sequential forward or backward selection. Sequential forward selection (SFS) sets out to compute a classification error for each feature and selects the vector of features that achieves the lowest classification error with minimal risk of overfitting.[26] The optimal number of features are chosen when the algorithm converged at the local minimum.

Embedded methods are a feature selection methods which finds the features that perform best during the training phase of the model and is a build-in function within the chosen model. Models that performs feature selection during training are boosting trees or random forest tree (RF).[26]

SFS and the embedded method were used in this study, however SFS did not improve the classification when used with the embedded method. Furthermore it was investigated if some of the features were providing misleading information. This was the case for features related to the gamma band. Signals in the gamma band differed from the rest of the frequency bands and would therefore always be chosen as the most important features during feature selection. The features provided a poor classification and it was not expected these would be chosen. However, after removing the gamma features, the feature selection methods would choose features which could be explained and gave a better performance. Features related to the gamma band were therefore excluded from further processing.

3.6 Classification and Evaluation

A channel-wise classification was conducted to detect and classify reaching and grasping movements. It was of interest to investigate how well the classifier was able to detect reaching and grasping from rest based on the seven subjects. Furthermore, it was of interest to investigate how well the chosen classifier perform in order to classify reaching and grasping based on session involving the two subjects. In the present study RF classifiers were evaluated for the detection and classification of reaching and grasping motions.

3.6.1 Decision Trees and Random Forest

Decision trees are a hierarchical tree-like model where the main components of the model are called nodes and leaf nodes. The model classifies each class label based on a series of logical conditions, either true or false statements, where each question is contained in a node. The decision tree starts from the top at the root node and then splitting the given training data into several subnodes based on the logical condition.[27, 28] Each subnode is called an internal node which contains a logical statement. The class is labelled when it reaches the leaf node which has no links to other internal nodes. Figure 3.11 illustrates an example of how a possible decision tree would be constructed for detecting reaching movement based on the slope of the fourth segment (S4) and the mean of the first segment in the alpha band (AM1). The nodes and subnodes are illustrated by the triangles whereas the circles are the leaf nodes which assigns the class label. If S4 is less than 2, the decision tree would label that sample as rest. However, if S4 is greater or equal to 2, an additional node will determine the outcome of the sample. If AM1 is greater or equal to 3, it would indicate this sample is associated with a movement, which would be the reaching movement in this example.

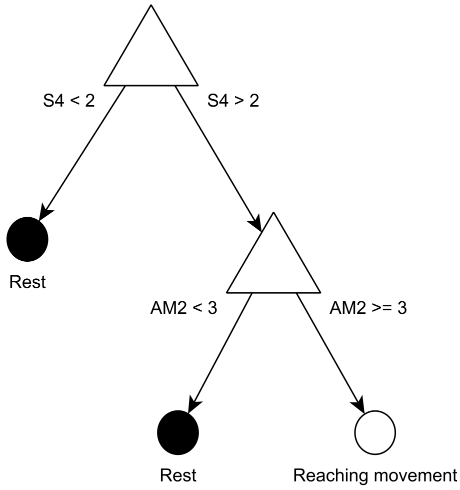

Figure 3.11: An example of how a decision tree possibly would be constructed for detecting reaching. The nodes and subnodes are illustrated as the triangles and are related to the features whereas the leaf nodes are the solid dots which indicates the target labels.

Ideally, the perfect split is when the training set can be classified based on one question. Based on this the classifier would label the training set as clean as possible. A measure of how pure the node classifies the training data in a node is given by the Gini index. The Gini index is a value between 0 and 1, where 0 indicates a high homogeneity of the training data, which is preferred, and 1 represents an inhomogeneous distribution of the class labels.[29] The Gini index is given by equation 3.2

$$i(N) = 1 - \sum_{i} P^2 \tag{3.2}$$

where i(N) is the impurity measure for node N and P is the probability of a class falling into the node N. The Gini index is a sum of squared measure of the likelihood a class will fall into a node. Since each node represents a feature, the Gini index can be used to illustrate the importance of each feature.[29, 27]
However, a problem with the decision tree model is its high variance. An instability of the hierarchical tree structure can affect the classification due to a small change in the data set. Growing deep trees increases the complexity of the model and also adds the risk of overfitting the data. Several methods can be applied to avoid overfitting such as pruning the leaf size or build a less complex tree model.[30] However, another approach can be applied, which is a RF classifier. RF is an ensemble classifier which sometimes achieves a higher performance than simple classifiers such as, linear discriminant analysis (LDA), support vector machine (SVM) and k-nearest neighbor[31]. However, in regards to the no free lunch theorem, there is no universally best machine learning model. A common standard is therefore to test several classifiers for the given classification problem.[31] In this study RF outperformed regularized LDA and SVM classifiers. The results of the LDA and SVM classification can be seen in appendix D and E.

In RF, several decision trees are built and each decision tree predicts on several bootstrapped training sets from the original training set and thereby "votes" for a class. The class with most votes is chosen as the final prediction. For each decision tree, a subset of features are randomly selected. The implementation of RF was based on the Classification and Regression Trees (CART) method proposed by Breiman[32]. The decision trees were grown to maximum size by setting the leaf size to 1[32]. Increasing the number of leaf size can potentially reduce the classification accuracy on large data sets. It was previously mentioned that a deep decision tree is prone to overfit, however it is not the case for a RF model, as it takes several decision trees into consideration and therefore reduces the variance[32]. Furthermore the number of features randomly selected in each node was set to be square root of the total amount of features. The total amount of features were 66 for each channel. The number of features for to create the best split was therefore nine features in each tree.[33] When performing a RF classification it is not necessary to apply a cross-validation scheme. RF holds out 1/3 of the data set as test set and estimates an unbiased classification error called out-of-bag (OOB) error. In order to get an unbiased error estimation, it is suggested to grow decision trees past the point where the OOB error converges. [32] It was investigated how many trees which were necessary for both objective. For the classification between reaching and grasping, the optimal number of trees was set to 800. For the detection of reaching and grasping, the optimal number of trees was set to 300. In general there is no rule of thumb for how many trees should be generated, but a large number of trees gives a stabilized OOB error and feature importance.[32] The optimal number of trees were found when the OOB error was lowest and did no longer improve.

3.7 Model Generation

The channel-wise classification was carried out by finding the channel that generalized best. The average OOB error was calculated for each channel. The channel with the lowest average OOB error was chosen as it was assumed it generalized well. Figure 3.12 illustrates the process of how each channel was used to train the classifier. The remaining eight channels were then used as unseen data to measure the performance metrics. This process was done for both objectives, respectively detection of reaching and grasping, and the classification of reaching and grasping.

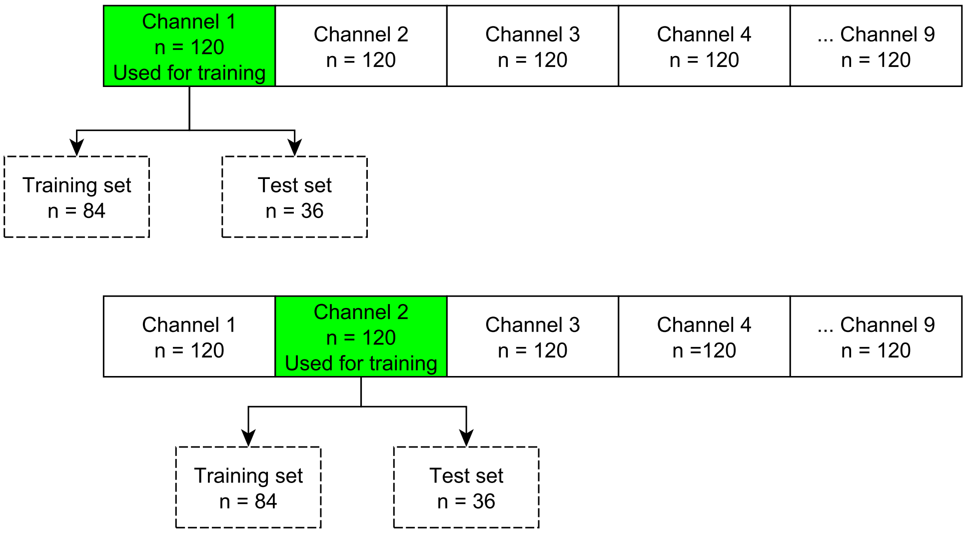

Figure 3.12: The process of building the optimal classifier was done through these steps. First channel 1 was used as training data to train the classifier. The channel was furthermore split into training and test where the RF model hold 1/3 of the data out as test set. The average out-of-bag error from each channel was used to evaluate how well the classifier generalized. This process was completed when all nine channels had been used as training. The channel with minimum average out-of-bag error was chosen. N is the number of epochs.

3.7.1 Evaluation Metrics

The performance of the RF classifier were evaluated on each channel which were used as unseen test data. To evaluate the classification performance of each channel, following evaluation metrics were used.

Accuracy

The accuracy of the classifier determines how well the classifier correctly classifies the two classes, for instance the reaching movement and rest. Accuracy is given by equation 3.3 [34]

$$Acc = \frac{TP + TN}{TP + TN + FP + FN} \tag{3.3}$$

where TP and TN are true positives and true negatives, where FP and FN are false positives and false negatives. It is the ratio of correct predictions over the total amount of all cases.[34]

Error Rate

Error rate illustrates how often the classifier is wrong and it is given by equation 3.4.[34]

$$Error = \frac{FP + FN}{TP + FP + TN + FN} \tag{3.4}$$

The error rate is also called the misclassification error and is the opposite of the accuracy. It measaures the ratio of incorrect predictions over the total amount of all cases.[34]

Sensitivity

Sensitivity is a measure of the correctly identified TP compared to FN For instance when it is detecting reaching, how often does it classify reaching correctly. Sensitivity is given by equation 3.5. [34]

$$Sensitivity = \frac{TP}{TP + FN} \tag{3.5}$$

Specificity

Specificity measures the opposite of sensitivity. It measures the fraction of correctly identified TN. Specificity is given by equation 3.6. [34]

$$Specificity = \frac{TN}{TN + FP} \tag{3.6}$$

Precision

Precision is a metric which is used to measure the amount of correctly predicted cases out of all the positive predictions and is given by equation 3.7.[34]

$$Precision = \frac{TP}{TP + FP} \tag{3.7}$$

4 | Results

In this chapter, the performance of the RF model will be presented along with the feature importance for each subject. First the performance of detecting reaching and grasping within the seven subjects will be presented along with their feature importance. Afterwards the performance of how well the model can classify reaching and grasping will be presented together with the feature importance of the two subjects who participated in session three.

4.1 Detection of Reaching and Grasping

The results of the RF classification for detecting reaching and grasping for the seven subjects can be seen in table 4.1 and 4.2. The tables show the average performance metrics and their standard deviation and indicates the performance of detecting reaching is slightly higher than detecting grasping by achieving an average TPR of 90.63% ± 18.43% (mean ± standard deviation) for all seven subjects. Overall, the percentage of error estimation for detecting reaching and grasping are respectively, 8.04% ± 11.61% and 10.63% ± 12.52%.

Table 4.1: The average obtained performance metrics for detecting reaching movement for the seven subjects. Abbreviations: Acc. = Accuracy, Sens. = Sensitivity, Spec. = Specificity, Prec. = Precision.

Detection of reaching				
Acc. (%)	**Sens. (%)**	**Spec. (%)**	**Prec. (%)**	**Error (%)**
91.96 ± 11.61	90.63 ± 18.43	94.29 ± 8.54	95.75 ± 5.64	8.04 ± 11.61

Table 4.2: The obtained average performance metrics for detecting grasping movement for the seven subjects. Abbreviations: Acc. = Accuracy, Sens. = Sensitivity, Spec. = Specificity, Prec. = Precision.

Detection of grasping				
Acc. (%)	**Sens. (%)**	**Spec. (%)**	**Prec. (%)**	**Error (%)**
89.37 ± 12.52	84.72 ± 21.76	95.15 ± 7.94	95.37 ± 8.12	10.63 ± 12.52

Figure 4.1 and 4.2 shows the feature importance for each subject in regards to the detection of reaching and grasping, respectively. The most important features were related to the frequency powerbands, delta, theta, alpha and beta, which all are important wavebands during voluntary movements. For an explanation of the features, see appendix C.

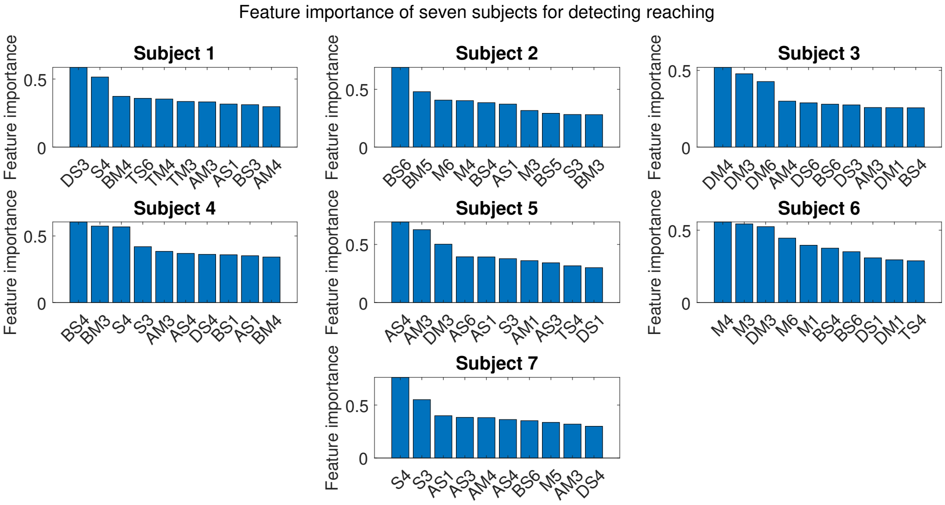

Figure 4.1: Top ten most important features for the seven subjects that were provided prior the study for detecting reaching movement. The y-axis is the feature importance which is given by the Gini index and the features are along the x-axis. The top ten features are mainly dominated by features from the powerbands.

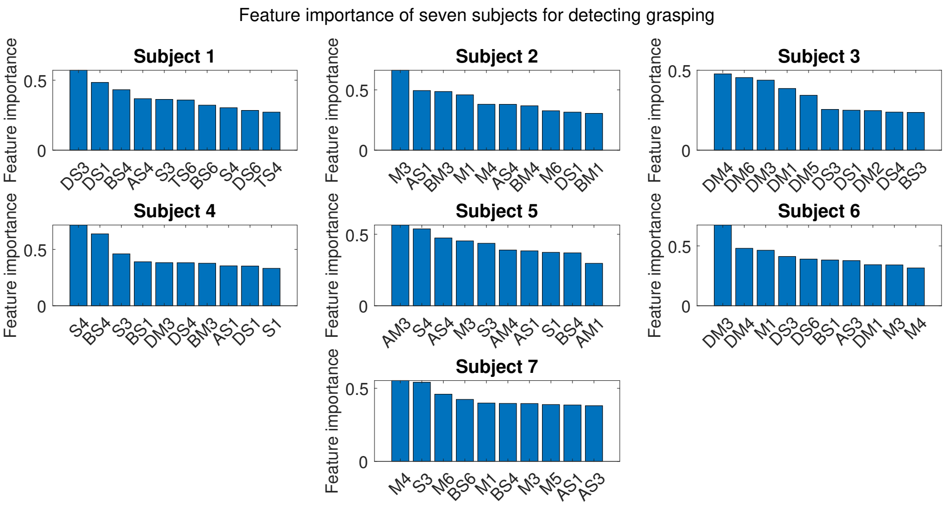

Figure 4.2: Top ten most important features for the seven subjects that were provided prior the study for detecting grasping. The y-axis is the feature importance which is given by the Gini index and the features are along the x-axis. For the detection of grasping, the most important features are a mix between features from the time domain and the powerbands.

4.1.1 Channel-wise Performance

Figure 4.3 and 4.4 shows the overall performance metrics for all seven subjects for the detection of reaching and grasping. The channel F3 is the worst performing channel in both detection algorithms in contrast to the other channels which achieves an overall accuracy >85%. Overall each channel achieves an acceptable performance.

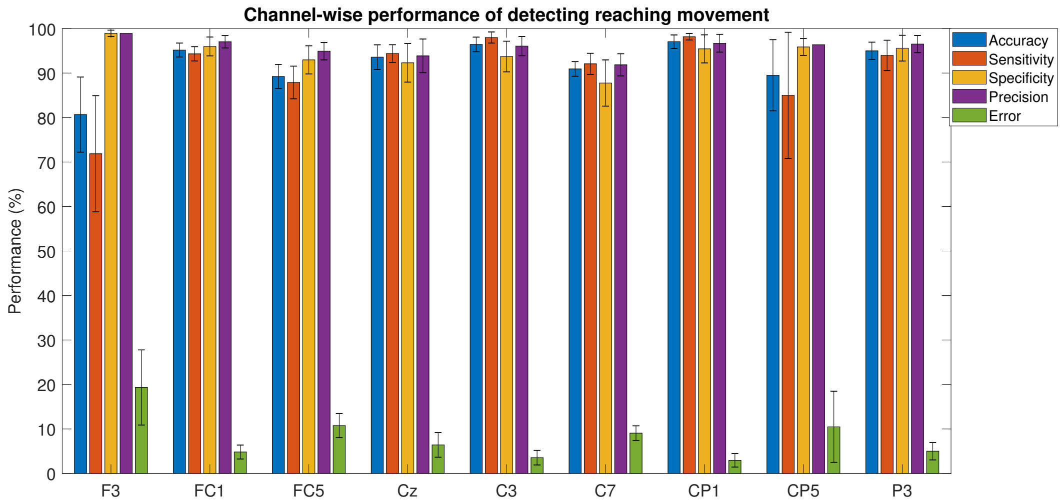

Figure 4.3: The overall average performance metrics for all seven subjects for each channel when detecting the reaching movement. The standard error of the mean is indicated by the error bars.

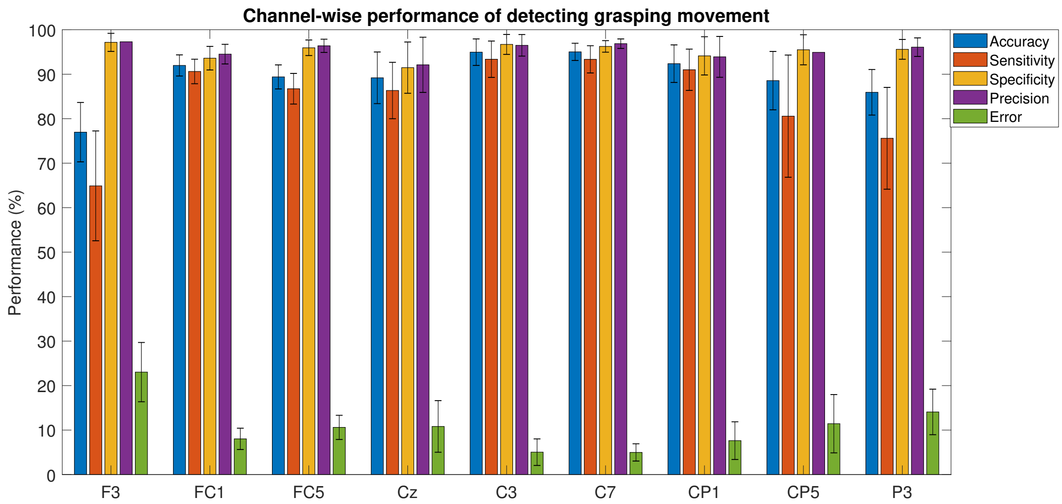

Figure 4.4: The overall average performance metrics for all seven subjects for each channel when detecting the grasping movement. The standard error of the mean is indicated by the error bars.

4.2 Classification of Reaching and Grasping

Table 4.3 shows the performance metrics of the data set consisting of reaching and grasping features for the two subjects. The average performances of the RF classification were obtained by averaging the performances for both subjects across all channels. The classification accuracy of reaching and grasping was 74.82% which indicates the classifier fails to classify between the two movements in 25.18% of the cases.

Table 4.3: The average results for both subjects for the classification of reaching and grasping using a Random Forest model. Abbreviations: Acc. = Accuracy, Sens. = Sensitivity, Spec. = Specificity, Prec. = Precision.

Classification of reaching and grasping				
Acc. (%)	**Sens. (%)**	**Spec. (%)**	**Prec. (%)**	**Error (%)**
74.82 ± 11.44	72.69 ± 13.13	77.13 ± 10.63	76.39 ± 11.09	25.18 ± 11.44

Feature importance of both subjects were derived and are shown in figure 4.5. The most important feature for subject 1 was the slope of the fourth segment (S4) and the most important feature for subject 2 was the mean of the first segment in the theta band (TM1). The top ten features for subject 1 was a mix between temporal and frequency features, whereas the top ten features for subject 2 consisted mainly of features from the power bands.

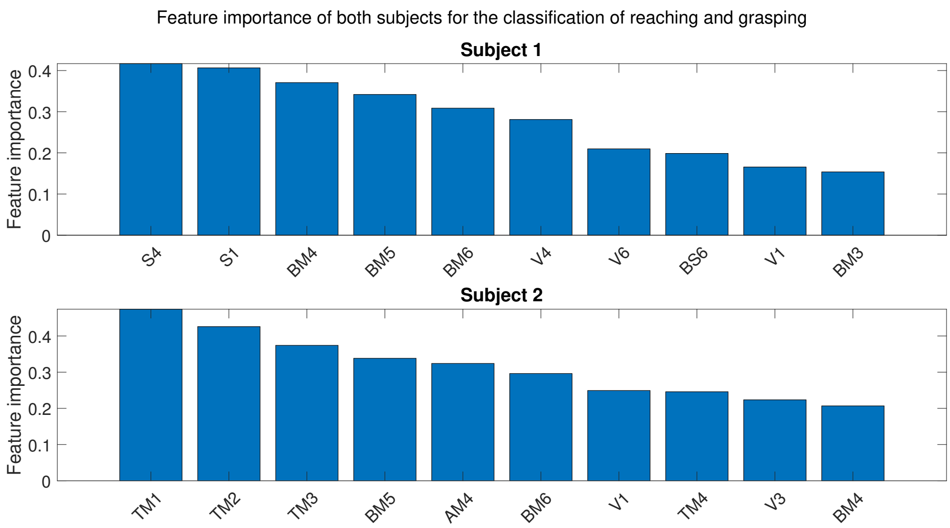

Figure 4.5: Top ten most important features for subject 1 and 2 when classifying reaching and grasping. The most important feature for subject 1 was the slope of the fourth segment (S4) and the most important feature for subject was the mean of the first segment in the theta band (TM1). The y-axis is the feature importance which is given by the Gini index and the features are along the x-axis.

Additionally, the performance of classification of movement (reaching and grasping) and rest was investigated. Table 4.4 shows the performance metrics and it illustrates that the model achieves an average accuracy of 94.73% when predicting movement and rest. The performances were obtained by the average of both subjects across all channels.

Table 4.4: The average results for both subjects for the classification of movement (reaching and grasping) and rest using a Random Forest model. Abbreviations: Acc. = Accuracy, Sens. = Sensitivity, Spec. = Specificity, Prec. = Precision.

Classificatin of movement and rest				
Acc. (%)	**Sens. (%)**	**Spec. (%)**	**Prec. (%)**	**Error (%)**
94.73 ± 3.73	96.14 ± 4.03	90.18 ± 10.46	96.78 ± 3.13	5.27 ± 3.73

Feature importance for the classification of movement and rest is illustrated in figure 4.6. The most important feature for subject 1 is the slope of the third segment (S3) whereas the most important feature for subject 2 was the variance in the first segment (V1). Furthermore it is seen the most important features were associated with steep slopes around the MRCP's which mainly are the segments 1,3,4 and 6.

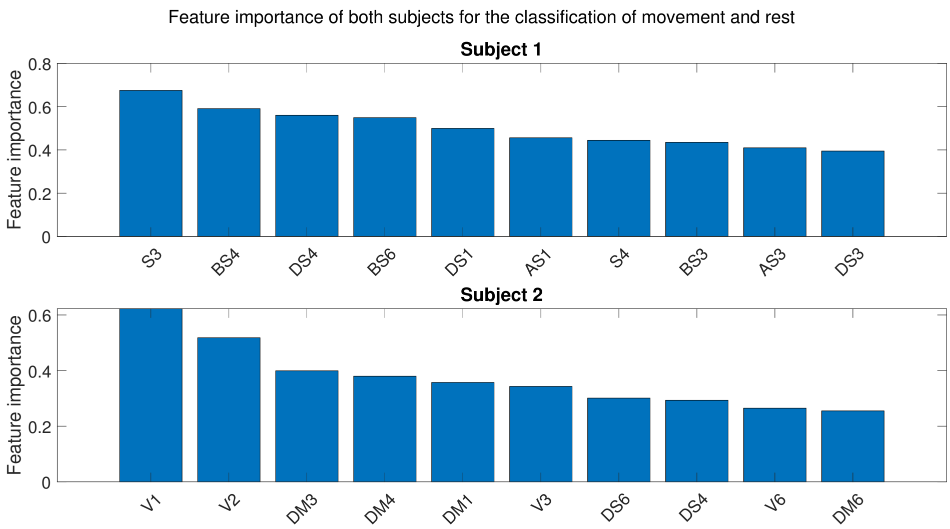

Figure 4.6: Top ten most important features for subject 1 and 2 when classifying movement and rest. The most important feature for subject 1 was the slope of the third segment (S3) and the most important feature for subject was the variance of the first segment (V1). The y-axis is the feature importance which is given by the Gini index and the features are along the x-axis.

4.2.1 Channel-wise Performance of the Classification of Reaching and Grasping movement

A channel-wise performance was carried out in order to investigate which channels performed best. Figure 4.7 shows the overall average performance metrics for both subjects together with the standard error of the mean. It is illustrated that channel FC5 achieved the highest accuracy 90.25% ± 9.75% and channel Cz achieved the lowest accuracy 63.02% ± 2.23%.

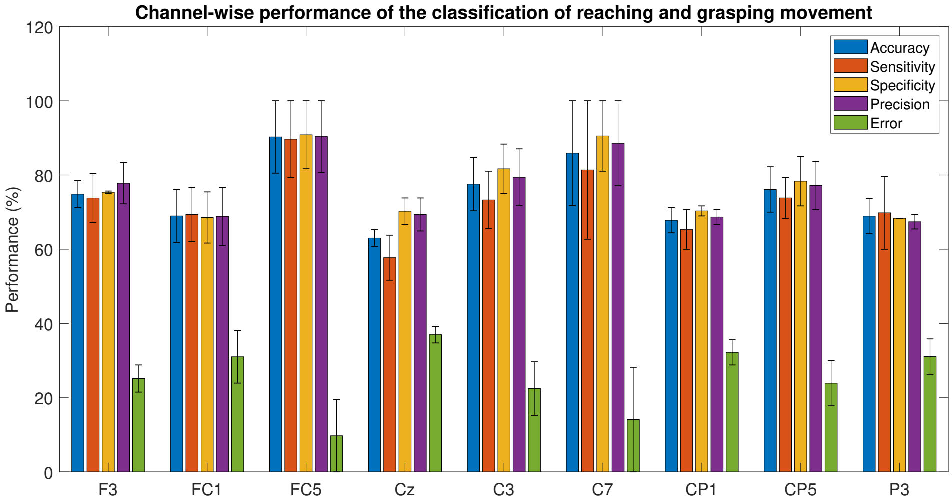

Figure 4.7: The overall average performance metrics for both subjects for each channel when classifying reaching and grasping movement. The standard error of the mean is indicated by the error bars.

5 | Discussion

In this chapter the aim will be summarized along with the most prominent results obtained from the individualized RF models. The results will thereafter be compared in regards to other studies which investigated detection or classification of MRCPs. Afterwards, the following sections will discuss the limitations and future research.

This study proposes a novel approach in order to achieve an accurate RF classification model. The chosen model is a RF, which has several advantages. First, it has a high predictive power and outperfoms the common classifiers used in BCI applications which are LDA and SVM. RF is gradually becoming more popular in machine learning applications due to its predictive power. Secondly, it is robust to outliers and noise. Even though outliers were removed, the model will be robust towards outliers in future data sets. Third, it obtains feature importance through the embedded method. Sequential forward selection was also implemented together with the embedded approach, however it did not improve the performance. Fourth, it is robust to overfitting due to reducing the high variance and low bias trade-off by depending on the outcome of several decision trees and also due to the bootstrapping approach within the model. According to the aim, which was to develop a MRCP-based BCI system in order to detect and classify reaching and grasping, it was possible to detect reaching and grasping. The average TPR for detecting reaching and grasping were 90.63% ± 18.43% and 89.72% ± 21.76% and 74.82% ± 11.44% for the classification of reaching and grasping. The results indicate that the model was able to detect reaching and grasping from rest with an acceptable accuracy. However, when classifying the two movements, it is more complicated. This was due to the two movements having similar MRCP shapes. Characteristics such as the maximum peak negativity can be of help when classifying the two movements. A complex movement such as reaching, has a tendency to have a more deep peak negativity than a simple movement such as grasping but it was not always the case for all channels, which explains why the RF model has an error of 25.18% ± 11.44% when classifying the two movements when all channels are taken into consideration. The feature importance revealed the most prominent features were features related to the segments associated with the steep slopes surrounding the MP, which was expected. The important features were generally the segments 1,3,4 and 6 and their slopes and means in both the time domain and in the delta, theta, alpha and beta bands. These features proves to be useful when it comes to classify reaching and grasping, which has similar shapes in MRCP. Small deviations in the features between these two movements can potentially be captured through the features associated with steep slopes around the MP. Variance were only important for detection of movement and rest. Additionally, this study is the first to classify reaching and grasping motions, in order to be utilized by ALS patients for control of a robotic arm.

5.1 Comparison with Similar Research

The majority of the literature regarding MRCP-based BCI systems focuses on detection of MRCP or classification of different hand movements such as lateral grasp, palmar grasp and pinch. Currently no study has investigated the relationship between a reaching motion and grasping motion. However, the detection of reaching and grasping can be compared to other studies which investigated the detection of grasping and reaching motions. A study by Jochumsen et al. [25] perfomed a three-class classification of palmar grasp, lateral grasp and pinch. The study proposed a LDA classifier which achieved an overall classification accuracy of 48% ± 5% (mean ± standard deviation) for the grasping movements. Grasping motions have similar shapes in regards to the slopes surrounding the MP of the MRCP, which may explain why the study achieves a low classification accuracy of 48% when classifying three grasping movements. Furthermore, the study derived feature importance based on sequential feature selection and illustrated the most important features came from the delta power band, which is in accordance to the results from this study. The frequency range of the MRCP is between 0.05-3 Hz, whereas the frequency range of the delta band is between 0.01-3 Hz. This may explain why the delta band is one of the most prominent features, because its frequency ranges are related to the MRCPs.
Niazi et al.[17] and Xu et al.[22] investigated MRCPs in ankle dorsiflexion. Niazi et al.[17] proposed a matched filter for detecting MRCPs related to ankle dorsiflexion and Xu et al.[22] proposed a Locality Presevering Projection followed by a LDA classifier(LPP-LDA). The detection performance for both studies were respectively 82% ± 7.8% and 84% ± 9.98% for motor execution in healthy subjects. In this study the average TPR were 90.63% ± 18.43% and 84.72% ± 21.76% for reaching and grasping motion respectively. The TPR are slightly higher compared to the two studies, however the standard deviations indicates a wide spread in the variance compared to the other studies, which indicates that the movement detection was poor for some subjects. Furthermore, the feature importance which were derived from this channel, may not represent the other channels that well. This could lead to some channels achieving a lower performance. The best channels to record MRCPs for hand movements are according, to Shakeel et al.[35], channel C1 and C2 as the BP2 is steepest in these channels. In this study channel F3, FC1, FC5, Cz, C3, T7, CP1, CP5, P3 were used and it was seen during training, that the channels which had the lowest OOB error was FC5 for subject 1 and C7 for subject 2 when performing classification of reaching and grasping. This may explain why these channels have a higher performance than the rest of the channels, since the classifiers for each subjects was built upon the channel which had the lowest OOB error. However, almost every channel achieved high performances when detecting reaching and grasping, except from F3 which had the lowest accuracy in both cases. Caution has to be advised when using a single channel to train the classifier as the feature importance from

single channels may not represent all channels due to different shapes of MRCPs occuring across the channels.
Furthermore another study by Ibanez et al.[36] proposed a logistic regression model to combine a Bayes classifier (which detected ERD) and a matched filter (which detected the BP) for detecting reaching motion in both healthy and stroke subjects. The performance of detecting reaching motions had on average a TPR of 82.2% ± 10.4% for the healthy subjects. In comparison to the results from this study, the performance of the reaching movement had on average an accuracy of 90.63% ± 18.43% across the seven subjects.

Most studies in the field of BCI proposes simple models, such as LDA, SVM and matched filter. This is due to the models having a fast computation time for online classification, hence the choice of more simple models than complex ones. However, complex models can sometimes achieve a higher accuracy but in contrast to computation time, it is slightly more computational heavy. Simple models are also robust in terms of hyperparameters as there are few parameters to tune in contrast to complex models. However, simple models are less robust towards outliers if their hyperparameters are not optimized, where complex models such as RF can handle outliers. In this study RF outperformed LDA and SVM which both were regularized. The RF models were regularized through instructions from Breiman [32]. The number of trees were decided based on visually inspecting where the OOB error converged for each channel. It was a general pattern that the OOB error converged between 80-100 trees for detection whereas the OOB converged at approximately 400 trees when classifying reaching and grasping for each channel.

5.2 Limitations and Future Research

A limitation in this study is that the online evaluation has not been done for the proposed RF model. The performance in offline classification has a high accuracy, however it would have been interesting to see to what extent the model would be accurate in an online classification. The performance of offline classification may not have the same performance as in an online classification. A simulation of online classification could have been performed by applying a sliding window on the subjects. Furthermore, the subjects which participated in the study were all able-bodied. The proposed MRCP-based BCI system is intended for patients suffering from ALS, it could therefore be ideal to have performed the same methodology on motor imagination as motor imagery differs from motor execution in regards to MRCP. With actual motor movement, the components of the MRCP are more apparent than in motor imagination, which is illustrated in figure 2.4.

6 Conclusion

The aim of this study was to investigate the detection performance of reaching and grasping and classification of reaching and grasping. Data sets from seven subjects were used for detection and data sets for two subjects were used for classification. By proposing a random forest classifier it was possible to both detect and classify reaching and grasping. The overall average TPR of the seven subjects for the detection of reaching and grasping were 90.63% ± 18.43% and 84.72% ± 21.76%. The overall classification accuracy of the two subjects for classification of reaching and grasping across all nine EEG channels was 74.82% ± 11.44%. Results from the feature importance indicated features derived from the powerband of the delta, theta, alpha and beta brain waves had a higher importance than features derived from the time domain. However, further investigation is needed in order to determine the usage of the model for real-time control of robotic arms for ALS patients.

Bibliography

[1] I. Lazarou, S. Nikolopoulos, P. C. Petrantonakis, I. Kompatsiaris, and M. Tsolaki, "EEG-Based Brain–Computer Interfaces for Communication and Rehabilitation of People with Motor Impairment: A Novel Approach of the 21st Century," *Frontiers in Human Neuroscience*, vol. 12, no. January, pp. 1–18, 2018.

[2] J. R. Wolpaw, G. Pfurtscheller, D. J. McFarland, N. Birbaumer, and T. M. Vaughan, "Brain-computer interfaces for communication and control," 2002.

[3] N. Birbaumer, "Breaking the silence: Brain-computer interfaces (BCI) for communication and motor control," *Psychophysiology*, vol. 43, no. 6, pp. 517–532, 2006.

[4] P. Couratier, P. Corcia, G. Lautrette, M. Nicol, P. M. Preux, and B. Marin, "Epidemiology of amyotrophic lateral sclerosis: A review of literature," *Revue Neurologique*, vol. 172, no. 1, pp. 37–45, 2016.

[5] L. F. Nicolas-Alonso and J. Gomez-Gil, "Brain computer interfaces, a review," *Sensors*, vol. 12, no. 2, pp. 1211–1279, 2012.

[6] F. H. Martini, J. L. Nath, and E. F. Bartholomew, *Fundamentals of human anatomy and physiology.*

[7] S. Ackerman, N. Academy, S. Isbn, T. Pdf, N. A. Press, N. A. Press, N. Academy, N. Academy, and N. A. Press, *Discovering the Brain.* 1992.

[8] https://www.actorsproexpo.com/uncategorised/top-5-tips-good-mental-health/attachment/brain-1007686$_9$60$_7$20, 2016. [*Accessed*02.01.19].

[9] J. G. Betts, *Anatomy & physiology.* 2013.

[10] L. Kinsley and T. Siddique, "Amyotrophic Lateral Sclerosis Overview," 2001.

[11] M. C. Kiernan, S. Vucic, B. C. Cheah, M. R. Turner, A. Eisen, O. Hardiman, J. R. Burrell, and M. C. Zoing, "Amyotrophic lateral sclerosis," *The Lancet*, vol. 377, no. 9769, pp. 942–955, 2011.

[12] S. Martin, A. Al Khleifat, and A. Al-Chalabi, "What causes amyotrophic lateral sclerosis?," *F1000Research*, vol. 6, no. 0, p. 371, 2017.

[13] R. A. Ramadan and A. V. Vasilakos, "Brain computer interface: control signals review," *Neurocomputing*, vol. 223, no. August 2016, pp. 26–44, 2017.

[14] L. E. van Dokkum, T. Ward, and I. Laffont, "Brain computer interfaces for neurorehabilitation-its current status as a rehabilitation strategy post-stroke," *Annals of Physical and Rehabilitation Medicine*, vol. 58, no. 1, pp. 3–8, 2015.

[15] D. Zhu, J. Bieger, G. Garcia Molina, and R. M. Aarts, "A survey of stimulation methods used in SSVEP-based BCIs," *Computational Intelligence and Neuroscience*, vol. 2010, 2010.

[16] G. Pfurtscheller and F. H. Lopes Da Silva, "Event-related EEG/MEG synchronization and desynchronization: Basic principles," *Clinical Neurophysiology*, vol. 110, no. 11, pp. 1842–1857, 1999.

[17] I. K. Niazi, N. Jiang, O. Tiberghien, J. Nielsen Feldbæk, K. Dremstrup, D. Farina, and N. Mrachacz-Kersting, "Detection of movement intention from single-trial movement-related cortical potentials," *Biosystems and Biorobotics*, vol. 7, pp. 237–244, 2014.

[18] H. Shibasaki and M. Hallett, "What is the Bereitschaftspotential?," *Clinical Neurophysiology*, vol. 117, no. 11, pp. 2341–2356, 2006.

[19] G. R. Müller-Putz and G. Pfurtscheller, "Control of an electrical prosthesis with an SSVEP-based BCI," *IEEE Transactions on Biomedical Engineering*, vol. 55, no. 1, pp. 361–364, 2008.

[20] G. Pfurtscheller, C. Guger, G. Müller, G. Krausz, and C. Neuper, "Brain oscillations control hand orthosis in a tetraplegic," *Neuroscience Letters*, vol. 292, no. 3, pp. 211–214, 2000.

[21] Han Yuan and Bin He, "Brain-Computer Interfaces Using Sensorimotor Rhythms: Current State and Future Perspectives," *IEEE Transactions on Biomedical Engineering*, vol. 61, no. 5, pp. 1425–1435, 2014.

[22] R. Xu, N. Jiang, C. Lin, N. Mrachacz-Kersting, K. Dremstrup, and D. Farina, "Enhanced low-latency detection of motor intention from EEG for closed-loop brain-computer interface applications," *IEEE Transactions on Biomedical Engineering*, vol. 61, no. 2, pp. 288–296, 2014.

[23] N. A. Bhagat, A. Venkatakrishnan, B. Abibullaev, E. J. Artz, N. Yozbatiran, A. A. Blank, J. French, C. Karmonik, R. G. Grossman, M. K. O'Malley, G. E. Francisco, and J. L. Contreras-Vidal, "Design and optimization of an EEG-based brain machine interface (BMI) to an upper-limb exoskeleton for stroke survivors," *Frontiers in Neuroscience*, vol. 10, no. MAR, 2016.

[24] C. Kamarajan, A. K. Pandey, D. B. Chorlian, N. Manz, A. T. Stimus, A. P. Anokhin, L. O. Bauer, S. Kuperman, J. Kramer, K. K. Bucholz, M. A. Schuckit, V. M. Hesselbrock, and B. Porjesz, "Deficient event-related theta oscillations in individuals at risk for alcoholism: A study of reward processing and impulsivity features," *PLoS ONE*, vol. 10, no. 11, 2015.

[25] M. Jochumsen, C. Rovsing, H. Rovsing, I. K. Niazi, K. Dremstrup, and E. N. Kamavuako, "Classification of Hand Grasp Kinetics and Types Using Movement-Related Cortical Potentials and EEG Rhythms," *Computational Intelligence and Neuroscience*, vol. 2017, 2017.

[26] Z. M. Hira and D. F. Gillies, "A review of feature selection and feature extraction methods applied on microarray data," *Advances in Bioinformatics*, vol. 2015, no. 1, 2015.

[27] Y.-y. Song and Y. Lu, "Decision tree methods : applications for classification and prediction," vol. 27, no. 2, pp. 130–135, 2015.

[28] C. Kingsford and Steven L Salzberg, "What are decision trees?," vol. 26, no. 9, pp. 1011–1013, 2009.

[29] R. Duda, P. Hart, and et.al, *Pattern Classification.* second edi ed., 2000.

[30] T. Hastie, R. Tibshirani, and J. Friedman, "The Elements of Statistical Learning," *The Mathematical Intelligencer*, vol. 27, no. 2, p. 83–85, 2001.

[31] R. Caruana and A. Niculescu-Mizil, "An Empirical Comparison of Supervised Learning Algorithms," pp. 161–168, 2006.

[32] L. Breiman, "Random Forests," pp. 5–32, 2001.

[33] L. Breiman, "Manual on setting up using and understanding Random Forests V4.0," pp. 1–33, 2017.

[34] H. M and S. M.N, "A Review on Evaluation Metrics for Data Classification Evaluations," *International Journal of Data Mining & Knowledge Management Process*, vol. 5, no. 2, pp. 01–11, 2015.

[35] Aqsa Shakeel, Muhammad Samran Navid, Muhammad Nabeel Anwar, Suleman Mazhar, Mads Jochumsen, and Imran Khan Niazi, "A Review of Techniques for Detection of Movement Intention Using Movement-Related Cortical Potentials," *Computational and Mathematical Methods in Medicine*, vol. 2015, p. 13, 2015.

[36] J. Ibáñez, J. I. Serrano, M. D. Del Castillo, E. Monge-Pereira, F. Molina-Rueda, I. Alguacil-Diego, and J. L. Pons, "Detection of the onset of upper-limb movements based on the combined analysis of changes in the sensorimotor rhythms and slow cortical potentials," *Journal of Neural Engineering*, vol. 11, no. 5, 2014.

[37] P. Xanthopoulos, P. M. Pardalos, and T. B. Trafalis, *Robust Data Mining.* 2012.

[38] C. F. Chao and M. H. Horng, "The construction of support vector machine classifier using the firefly algorithm," *Computational Intelligence and Neuroscience*, vol. 2015, 2015.

A | Neurons and Action Potentials

One of the building blocks of the brain are neurons. Neurons are electrically excitable cells, which receive, process and transmit information in the body through electrical and chemical signals. Neurons communicates with one another by sending electrochemical signals and thereby forming the basis of the brain's essential functions: to execute involuntary and voluntary movement, along with forming thoughts and memories and interpreting the world through visual, auditory and sensory information. The electrochemical signals are first being triggered in a neuron's axon. Axons are specialized to conduct electrical impulses that travels along the axon to its end at the axon's terminal. Axon terminals are connected with other neurons through synapses, in this way a single action potential can trigger a series of action potentials in multiple neurons simultaneously. There are two types of synapses; a chemical and an electrical synapse. In a chemical synapse, the action potential will cause the presynaptic cell to release neurotransmitters which are diffused across the synaptic cleft and binded to a receptor at the postsynaptic cell of another neuron. The binding of a neurostransmitter can induce a new action potential or inhibit the neuron, depending on the receptor at the postsynaptic cell. Electrical synapses triggers electrical impulses instead of neurotransmitters and occurs when the cell membrane of two neurons are close together.[6, 7]. If there are not any motorneurons to receive the action potential, voluntary movements may therefore not be triggered which leads to dysfunctions in executing voluntary movements, which is the case in ALS patients.

B | Brain Wavebands

EEG signals comprises a set of signals, which can be analyzed through frequency ranges. These frequency ranges have different frequency ranges across the scalp. EEG signals can be divided into five different frequency bands respectively, delta, theta, alpha, beta and gamma band.[5]

Delta band

The delta band frequency lies between 0.1 to 4 Hz and are slow waves which occurs in the deep stages of sleeping. If there is a elevated activity in the delta band in the waking state, it could be related to deficiencies in the brain.[5]

Theta band

The theta band frequency ranges from 4 to 7 Hz and elevated activity can be seen during mental tasks, such as math calculations.[5]

Alpha band

The alpha band waves, ranges from 8 to 12 Hz, and are generated across cortical regions including the occipital, parietal and temporal lobe. The amplitudes are decreased when the eyes are closed and attenuated when the eyes opens again. Furthermore the ampltiude of the waves can be elevated through mental tasks. Mental tasks, such as motor activity causes the alpha activity to be suppressed in the frontal lobe. Another frequency band can be found in the alpha band, which is called Mu rhythms. The differences between alpha and mu are that mu rhythms are high correlated with motor activities, where the maximum mu activity of the recorded over the motor cortex.[5]

Beta band

The beta band waves are located in the frequency range 12 and 30 Hz and can be found in both central and frontol regions of the brain. These waves are correlated with motor activities, where an executed movement or motor intention will cause a desynchronization in the beta band, which is seen as a suppression of the signal.[5]

Gamma band

Gamma waves are in the frequency range of 32 to 100 Hz and up. The gamma waves are related to motor functions and perceptions. However, it is not commonly used in BCI as the waves can be affected by artifacts from EMG and EOG.[5]

C | Feature Description

Table C.1: Features extracted based on the epochs from the time domain.

Feature	**Description**
M1	Mean of the first segment
M2	Mean of the second segment
M3	Mean of the third segment
M4	Mean of the fourth segment
M5	Mean of the fifth segment
M6	Mean of the sixth segment
V1	Standard deviation in the first segment
V2	Standard deviation in the second segment
V3	Standard deviation in the third segment
V4	Standard deviation in the fourth segment
V5	Standard deviation in the fifth segment
V6	Standard deviation in the sixth segment
S1	Slope of the first segment
S2	Slope of the second segment
S3	Slope of the third segment
S4	Slope of the fourth segment
S5	Slope of the fifth segment
S6	Slope of the sixth segment

Table C.2: Features extracted from the delta power band.

Feature	Description
DM1	Mean of the first segment in the delta band
DM2	Mean of the second segment in the delta band
DM3	Mean of the third segment in the delta band
DM4	Mean of the fourth segment in the delta band
DM5	Mean of the fifth segment in the delta band
DM6	Mean of the sixth segment in the delta band
DS1	Slope of the first segment in the delta band
DS2	Slope of the second segment in the delta band
DS3	Slope of the third segment in delta band
DS4	Slope of the fourth segment in the delta band
DS5	Slope of fifth segment in the delta band
DS6	Slope of the sixth segment in the delta band

Table C.3: Features extracted from the theta power band.

Feature	Description
TM1	Mean of the first segment in the theta band
TM2	Mean of the second segment in the theta band
TM3	Mean of the third segment in the theta band
TM4	Mean of the fourth segment in the theta band
TM5	Mean of the fifth segment in the theta band
TM6	Mean of the sixth segment in the theta band
TS1	Slope of the first segment in the theta band
TS2	Slope of the second segment in the theta band
TS3	Slope of the third segment in theta band
TS4	Slope of the fourth segment in the theta band
TS5	Slope of fifth segment in the theta band
TS6	Slope of the sixth segment in the theta band

Table C.4: Features extracted from the alpha power band.

Feature	Description
AM1	Mean of the first segment in the alpha band
AM2	Mean of the second segment in the alpha band
AM3	Mean of the third segment in the alpha band
AM4	Mean of the fourth segment in the alpha band
AM5	Mean of the fifth segment in the alpha band
AM6	Mean of the sixth segment in the alpha band
AS1	Slope of the first segment in the alpha band
AS2	Slope of the second segment in the alpha band
AS3	Slope of the third segment in alpha band
AS4	Slope of the fourth segment in the alpha band
AS5	Slope of fifth segment in the alpha band
AS6	Slope of the sixth segment in the alpha band

Table C.5: Features extracted from the beta power band.

Feature	Description
BM1	Mean of the first segment in the beta band
BM2	Mean of the second segment in the beta band
BM3	Mean of the third segment in the beta band
BM4	Mean of the fourth segment in the beta band
BM5	Mean of the fifth segment in the beta band
BM6	Mean of the sixth segment in the beta band
BS1	Slope of the first segment in the beta band
BS2	Slope of the second segment in the beta band
BS3	Slope of the third segment in beta band
BS4	Slope of the fourth segment in the beta band
BS5	Slope of fifth segment in the beta band
BS6	Slope of the sixth segment in the beta band

D | Linear Discriminant Analysis

LDA is a supervised classification method which is used to discriminate between two or more classes and to classify a new observation set into these known groups. It assumes the classes are linearly separable and defines a discrimination function which is given by equation D.1

$$g(x) = w^t x + w_0 \tag{D.1}$$

where w^t is a weight applied to the feature vector x, w_0 is a threshold weight and determines the location of the hyperplane and g(x) represents the hyperplane decision surface in the feature space. The hyperplane separates the classes depending on which side of the hyperplane the feature vector belongs to. Each feature is classified according to the g(x) value. If g(x)>0, x is on the positive side of the hyperplane and g(x)<0 when x is on the negative side.[29, 5] Furthermore the intuition of LDA is to maximize the separability of the two classes and projects the features into a lower dimensionality to minimize within class variance.[37] Separating two classes is useful, in this case separating reaching and grasping from resting. LDA is commonly used when implementing a BCI due to its low computational power and good accuracy. However, it is prone to overfit if the feature dimensionality is too high. To prevent overfitting, regularization is necessary. LDA has two hyperparameters, γ and δ. γ is a shrinkage parameter that is used to estimate the covariance matrix of the features. δ is a hyperparameter that is used to remove redundant features. The higher value the more features will be removed.[5] In order to build a robust LDA classifier, the hyperparameters was selected by performing a gridsearch together with a 5-fold cross-validation. A sequential forward selection was performed to find the best subset of features during training.
The results for detecting reaching and grasping can be seen in tableD.1 and D.2 respectively. The results for the classification of reaching and grasping can be seen in table D.3

Table D.1: The obtained performance for detecting reaching movement for the seven subjects using a LDA classifier. Abbreviations: Acc. = Accuracy, Sens. = Sensitivity, Spec. = Specificity, Prec. = Precision.

Detection of reaching				
Acc. (%)	**Sens. (%)**	**Spec. (%)**	**Prec. (%)**	**Error (%)**
86.76 ± 9.06	91.54 ± 9.14	80.42 ± 15.02	86.42 ± 9.24	13.24 ± 9.06

Table D.2: The obtained performance for detecting grasping movement for the seven subjects using a LDA classifier. Abbreviations: Acc. = Accuracy, Sens. = Sensitivity, Spec. = Specificity, Prec. = Precision.

Detection of grasping				
Acc. (%)	**Sens. (%)**	**Spec. (%)**	**Prec. (%)**	**Error (%)**
86.84 ± 8.68	89.37 ± 10.13	82.16 ± 12.08	87.24 ± 7.57	13.16 ± 8.68

Table D.3: The obtained performance for the classification of reaching and grasping for the two subjects in session three using a LDA classifier. Abbreviations: Acc. = Accuracy, Sens. = Sensitivity, Spec. = Specificity, Prec. = Precision.

Classification of reaching and grasping				
Acc. (%)	**Sens. (%)**	**Spec. (%)**	**Prec. (%)**	**Error (%)**
68.83 ± 7.33	68.70 ± 9.09	68.90 ± 10.13	69.90 ± 7.64	31.17 ± 7.33

E | Support Vector Machine

SVM is a supervised classification method which is similar to LDA. It projects the features into a higher dimensional space and constructs a hyperplane to separate the classes, however instead of maximizing the class separability, it maximizes the distance between the nearest training sample and the hyperplane. In this way, SVM focuses on the points closest to the hyperplane in order to classify these, as they are difficult to classify in contrast to training samples further away. These difficult samples are close to the hyperplane and are called support vectors which also are the most informative points for the classifier. They define the maximal margin that is used to construct the optimal hyperplane.[29, 5] Figure E.1 illustrates how the optimal hyperplane is constructed using the support vectors.

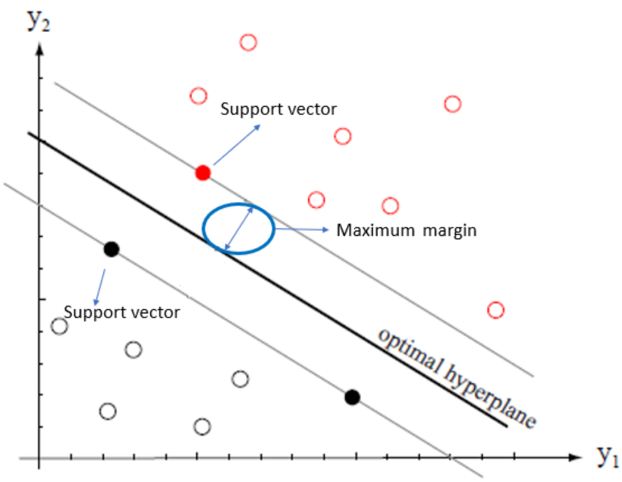

Figure E.1: A 2D representation of a SVM hyperplane. The solid dots are the support vectors with their equal maximum distance to the hyperplane. Modified from[29].

SVM classifiers are efficient and are robust in regards to the curse of dimensionality, however regularization is necessary to prevent misclassification of each sample and overfitting.[5] C is a hyperparameter that can be tuned through optimization. It determines how much the classifier misclassifies the samples by penalizing the size of the margin. The optimal hyperplane is when the largest margin is acquired. However, in reality it is not possible to achieve the largest margin meanwhile classifying each sample correctly. The C parameter is a trade-off between maximising the margin and classifying enough training samples. A high C value results in a small margin while a low C value results in a large margin.[38] A 5-fold cross validated gridsearch was performed to obtain the C parameter to obtain the lowest classification error. Furthermore, a sequential forward selection was performed to obtain the features for the SVM classifier. The results for detecting reaching and grasping can be seen in table E.1 and E.2 respectively. The results for the classification of reaching and grasping can be seen in table E.3

Table E.1: The obtained performance for detecting reaching movement for the seven subjects using a SVM classifier. Abbreviations: Acc. = Accuracy, Sens. = Sensitivity, Spec. = Specificity, Prec. = Precision.

Detection of reaching				
Acc. (%)	**Sens. (%)**	**Spec. (%)**	**Prec. (%)**	**Error (%)**
86.53 ± 10.57	93.52 ± 8.63	77.91 ± 20.38	85.74 ± 11.94	13.47 ± 10.57

Table E.2: The obtained performance for detecting grasping movement for the seven subjects using a SVM classifier. Abbreviations: Acc. = Accuracy, Sens. = Sensitivity, Spec. = Specificity, Prec. = Precision.

Detection of grasping				
Acc. (%)	**Sens. (%)**	**Spec. (%)**	**Prec. (%)**	**Error (%)**
90.03 ± 7.44	92.94 ± 9.24	86.78 ± 9.38	89.68 ± 7.01	9.97 ± 7.44

Table E.3: The obtained performance for the classification of reaching and grasping for the two subjects in session three using a SVM classifier. Abbreviations: Acc. = Accuracy, Sens. = Sensitivity, Spec. = Specificity, Prec. = Precision.

Classification of reaching and grasping				
Acc. (%)	**Sens. (%)**	**Spec. (%)**	**Prec. (%)**	**Error (%)**
70.87 ± 9.04	65.96 ± 15.24	75.52 ± 8.44	73.39 ± 8.29	29.13 ± 9.04